CellPress

Chem Catalysis

Review

Principles and applications of photothermal catalysis

Chuqiao Song,[1] Zhaohua Wang,[1] Zhen Yin,[2,*] Dequan Xiao,[3,*] and Ding Ma[1,*]

SUMMARY

Solar energy provides an alternative, sustainable, and clean source of energy to meet the global energy demands without extra carbon emissions. However, the utilization efficiency of sunlight via most traditional photocatalytic processes remains relatively low. Photothermal catalysis, combining the advantages of photocatalysis and thermocatalysis, has emerged as a new fast-growing research area. In this review, we first discuss three different mechanisms of photothermal effects and then describe the functioning principles of photothermal catalysis. We categorize the photothermal catalysts into three types based on their specific coupling modes of thermochemical and photochemical pathways. We also illustrate the catalyst design strategies and characterization methods for photothermal catalysis. As specific examples of applications, we summarize the recent research progress on the photothermal catalytic reactions for CO_2 conversion, CH_4 activation, NH_3 synthesis, and water splitting. Last, we present the challenges and perspectives in this field, as a guide for future development in photothermal catalysis.

INTRODUCTION

Global energy demand is rapidly increasing due to the growth of the world's population and substantial industrial production.[1,2] Currently, the traditional fossil fuels (oil, natural gas, and coal) still constitute the main source of energy consumption in the world (Figure 1A).[3] However, the tremendous consumption of fossil fuels can lead to severe environment issues and huge amounts of carbon emissions.[4] Hence, significant efforts have been devoted to the exploration and development of renewable energy,[5] such as solar,[6] wind, ocean, tidal, and wave energy. A rising trend in renewable energy sources has been demonstrated by the fast growth of renewable energy in recent years (Figure 1B).

Solar energy, as a type of abundant, clean, and renewable energy, has been widely used in various fields in the past decades, including desalination,[8] solar evaporation,[9] and photoelectric processes.[10] In 1972, a pioneering work was reported by Fujishima and Honda on a photoelectrochemical system composed of a TiO_2 photoelectrode and a platinum electrode for water splitting,[11] leading to the birth of a new research field: photocatalysis. Since then, the utilization of solar energy to drive heterogeneous catalytic reactions for fuels and chemicals has gained extensive attention as an environmentally friendly and promising alternative to traditional heterogeneous catalytic processes driven by thermal energy.[6,12] Although enormous research efforts have been devoted to semiconductor photocatalysis, two main challenges have greatly hindered the large-scale application of photocatalysis until now, namely weak absorption of sunlight in the visible and infrared (IR) regions and very low apparent quantum efficiency.[13,14]

The bigger picture

Sunlight harvesting and conversion is a challenging and active research area. Photothermal catalysis, as a promising technology, can dramatically enhance the catalytic activity and modulate the catalytic pathway due to a synergy between photochemical and thermochemical reaction pathways. It is pivotal to improving the photothermal catalytic conversion by exploring efficient photothermal catalysts with intense broadband solar energy absorption and high efficiency of solar-to-heat conversion. Understanding the synergy of light and heat underlying photothermal effects is of significant importance for enhancing photothermal catalytic performance. In this review, we present the functioning principles and categories of photothermal catalysis, catalyst design criteria and strategies, and recent progress in applying photothermal catalysis in several important reactions of heterogeneous catalysis.

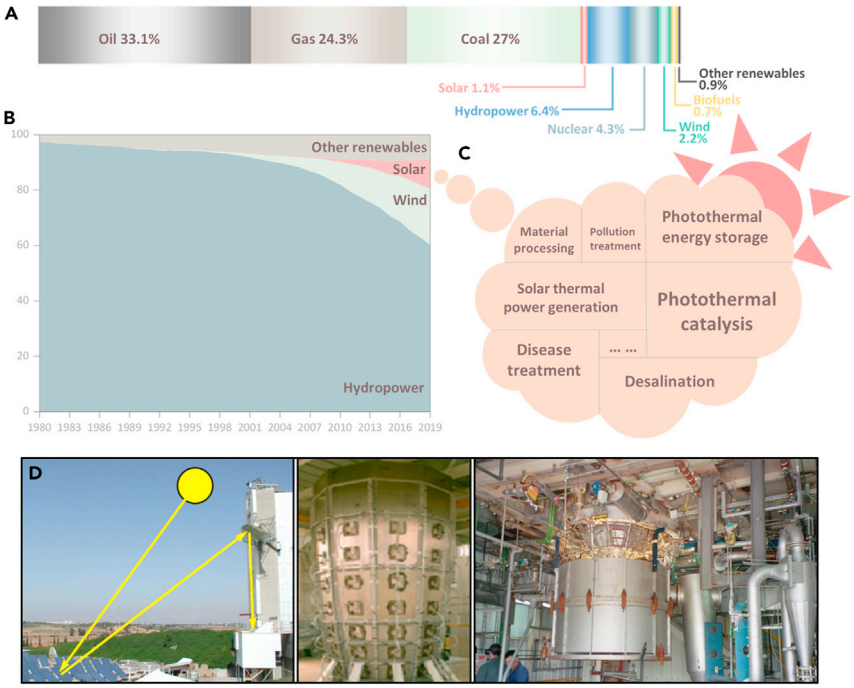

Figure 1. Current status of solar energy utilization

(A) Global primary energy consumption in 2019 by source (sources: BP Statistical Review of World Energy and Ember).[3]

(B) Modern renewable energy generation by source in world (sources: BP Statistical Review of World Energy and Ember).[3]

(C) Applications of photothermal effect.

(D) Compound parabolic concentrator (CPC) located in the upper level of the white container, above the pilot solar reactor (left); 300 kW pilot solar reactor with off-gas system for Zn dust production in operation (middle); solar tower at WIS (Weizmann Institute of Science, Israel) with beam-down optical system (right).[7]

Along with photocatalysis based on semiconductors, photothermal catalysis has become an exciting and fast-growing new research area in the past few years. Indeed, photothermal catalysis can combine the advantages of thermocatalysis and photocatalysis, thereby rendering excellent catalytic performance even under moderate conditions.[15] Meanwhile, we have witnessed the rapid growth of various innovative photothermal materials and their extensive applications in catalysis.[16]

In this review, we first introduce the fundamental principles of photothermal catalysis, including different mechanisms of photothermal conversion (i.e., plasmonic localized heating, non-radiative relaxation of semiconductors, and thermal vibration in molecules) and different types of photothermal catalytic processes. Subsequently, we discuss several typical photothermal catalysts and the design strategies of effective photothermal catalysts, including the hybrid structures of metal nanoparticles/semiconductors, metal nanoparticles/MOFs, and semiconductors/MOFs. Thereafter, we outline recent developments in various catalytic reactions, including CO_2 conversion, CH_4 activation, NH_3 synthesis, and water splitting. Last, the challenges and perspectives of photothermal catalysis are presented. The aim of this review is to offer enhanced understanding of photothermal catalysis and shed light on the design and potential applications of photothermal catalysts.

[1]Beijing National Laboratory for Molecular Sciences, College of Chemistry and Molecular Engineering and College of Engineering, and BIC-ESAT, Peking University, Beijing 100871, PR China

[2]College of Chemical Engineering and Materials Science, Tianjin University of Science and Technology, Tianjin 300457, PR China

[3]Center for Integrative Materials Discovery, Department of Chemistry and Chemical Engineering, University of New Haven, West Haven, CT 06516, USA

*Correspondence: yinzhen@tust.edu.cn (Z.Y.), dxiao@newhaven.edu (D.X.), dma@pku.edu.cn (D.M.)

https://doi.org/10.1016/j.checat.2021.10.005

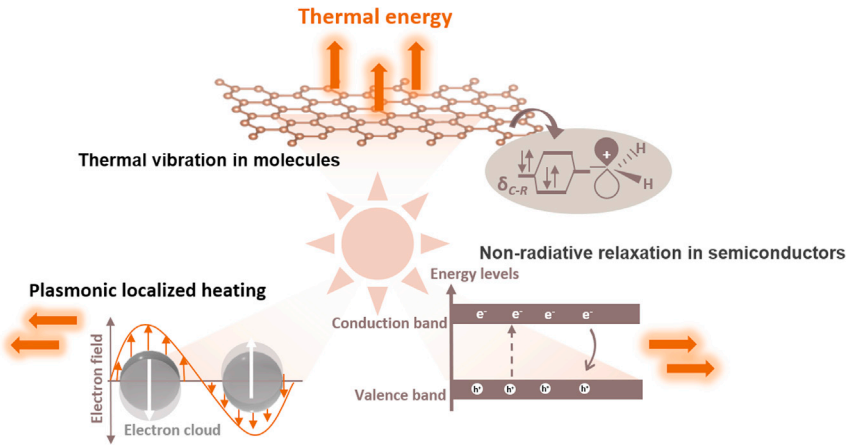

Figure 2. Different mechanisms of photothermal effect

A BRIEF OVERVIEW OF PHOTOTHERMAL CATALYSIS

Mechanism of photothermal effect

In fact, researchers are very familiar with the photothermal effect of sunlight, such as in the application of solar water heaters. In addition, there are photothermal power generation and photothermal energy storage device design (Figure 1C).[14,17,18] Particularly, intensive attempts and strategies have been devoted to realizing photothermal industrialization. Large-scale and highly concentrated solar systems, such as heliostat fields and towers, are expected to provide high-temperature conditions to drive thermal and thermochemical processes for fuel production, as well as some traditional industrial processes (Figure 1D).[7,19]

The photothermal effect has been widely observed in various photothermal materials, such as inorganic materials (e.g., plasmonic metals and semiconductors)[20,21] and organic materials (e.g., polymers)[22], which convert incident light into thermal energy (heat) under irradiation. A photothermal process is a direct conversion of solar light, which can exhibit maximally achievable efficiency of energy conversion compared with other solar energy utilization technologies. According to the interaction mechanisms of light and matter, three different photothermal mechanisms can be classified, namely, plasmonic localized heating, non-radiative relaxation in semiconductors, and thermal vibration of molecules (Figure 2).[17,23] Light may be converted into heat through one or more of these photothermal mechanisms in a particular photothermal material.

Plasmonic localized heating

Under external irradiation, the electromagnetic wave can induce collective oscillation of electrons at the interface between the conducting materials and a dielectric medium (e.g., air or water) when the light's frequency matches the resonant frequency of conduction band electrons. Such coherent electron oscillations can be confined on a subwavelength structure, which is referred to as surface plasmon resonance (SPR).[24] Since it is extremely localized, this phenomenon is sometimes called localized surface plasmon resonance (LSPR).[25] SPR excitation can lead to a dramatic enhancement of local electric fields and produce a high concentration of energetic (hot) electrons on the surface of a plasmonic structure.[26] After excitation (about 5–100 fs), the energy from SPR can decay via non-radiative (electron-electron collisions and electron-hole pair recombination) and radiative (re-emission of photons) pathways.[27] The plasmon decay via the non-radiative pathway can couple to phonon

modes by electron-phonon scattering and thereby heat up the metal lattice (100 fs to 1 ps). This heat can be dissipated to the surrounding environment (100 ps to 10 ns) through phonon-phonon relaxation. Hence, three different processes are involved in SPR: enhancement of local electric field, generation of hot electrons, and photothermal conversion.[26] The SPR can be observed in nanomaterials with high mobility of free electrons, such as Au, Ag, Cu, Al, and doped semiconductors.[28,29] More importantly, the SPR can be easily tuned in the entire visible and near-IR (NIR) region of the solar energy spectrum by manipulating the size, shape, and composition of plasmonic nanomaterials.[24] For example, the plasmon absorption peak of Au nanoparticles exhibited red shift with increasing particle diameter from 517 nm (for the 9 nm particles) to 575 nm (for the 99 nm particles).[30] Moreover, Au nanostructures can broaden the spectral range of SPR and change the mode of SPR by reducing shape symmetry. For example, Au nanorods possess longitudinal modes in the NIR region due to the plasmon oscillation of electrons along the long axis of the nanorods, in addition to transverse modes at shorter wavelengths. The SPR spectra of Au nanorods can be tuned by tailoring the aspect ratio.[31] For the bimetallic Au-Ag alloy nanoparticles, it was found that the SPR band showed a linear blue shift with increasing silver content.[32]

Non-radiative relaxation in semiconductors

In semiconductors, strong light absorption can be exhibited, with the light wavelength close to the band-gap energy. Photons with near or higher energy than the band gap can cause the generation of electron-hole pairs.[33] Then, the excited electrons can relax to the lower-energy states. The energy can be released through two mechanisms: non-radiative relaxation in the form of excited phonons and radiative relaxation through emitted photons. Due to the non-radiative relaxation process, local heating is produced via lattice vibration. However, the recombination of electrons and holes across the band gap can lead to energy loss through photon emission. Hence, the band-gap width of semiconductors can crucially determine the photothermal conversion efficiency.

For the semiconductors with narrow band gap, the energy of most photons from sunlight is higher than the band-gap energy, leading to the production of electron-hole pairs above the band gap. These electron-hole pairs can relax to band edges via the non-radiative relaxation pathway, releasing excess energy in the form of heat. In contrast, most of the photons with energy lower than the band-gap energy are scattered in the semiconductors with wide band gap, leading to extremely low efficiency of photothermal conversion.

Thermal vibration in molecules

Loosely held electrons can be excited from the ground state to the higher-energy orbitals when incident light energy matches the electronic transition energies in molecules. For example, the electron transition can occur from the highest occupied molecular orbital (HOMO) to the lowest unoccupied molecular orbital (LUMO) under irradiation. Then, the photoexcited electrons relax back to the ground state through the electron-vibration coupling, leading to heat generation in molecules. Carbonaceous[34] and some polymeric materials[35] (usually polymers with black color) with strong light absorption can convert solar energy into thermal energy through the thermal vibration mechanism due to their abundant conjugated π bonds, which can facilitate electron excitation from π to π^* orbitals even with low irradiation energy.[36] Furthermore, the energy gap between the LUMO and the HOMO can decrease when the number of π bonds increases.

By comparison, these three photothermal mechanisms can happen because of the nature of specific photothermal materials. For plasmonic localized heating, a large number of free electrons (e.g., electrons in the conduction bands of metals) are needed in order to induce coherent oscillation of electrons or surface plasmon resonance. Thus, this mechanism usually happens in metals or metallic nanostructures. The SPR will decay through non-radiative relaxation or photon re-emission. As a result, the oscillating electrons will return to the non-resonant ground state in the materials. For the non-radiative relaxation in semiconductors, no SPR effect is observed due to the lack of a large number of free electrons in semiconductors before irradiation. However, the electrons excited from the valence bands to the conduction bands will relax back the valence state via electron-phonon coupling. Hence, strong electron-phonon coupling is needed to facilitate the energy transfer from electrons to phonons, leading to the localized heating of semiconductors. In the mechanism of thermal vibration in molecules, the electrons are excited from the ground state to the excited state within the molecules, instead of the semiconductors or metals. After that, the excited electrons will relax back to the ground state via electron-vibration coupling, leading to the localized heating of the molecules. In this case, if the molecules were adsorbed on the surface of a metal or semiconductor, the separate mechanism of plasmonic localized heating (on metals) or non-radiative relaxation (on semiconductors) can exist simultaneously under the irradiation of solar light.

What is photothermal catalysis

Both light and heat are common sources for driving reactions in heterogeneous catalysis, where most catalytic reactions can occur via thermal catalytic processes, such as hydrogenation, oxidation, carbonylation, polymerization, halogenation, cracking, hydration, alkylation, isomerization, and other reactions.[37–39] Since thermal energy can be easily obtained through the combustion of fossil fuels, most industrial catalytic reactions are driven by thermal energy, such as the Haber-Bosch process (ammonia synthesis),[40] Fischer-Tropsch synthesis,[41] CO_2 hydrogenation to methanol,[42] and water-gas shift (WGS) reaction.[43] However, the high energy demand and rapid consumption of fossil fuels, as well as the environmental issues induced by carbon emissions, have made traditional thermal catalytic processes undesirable in the long run. Hence, it is highly desirable to seek green, mild, and sustainable ways to drive catalytic reactions.

Functioning principles of photothermal catalysis

Generally speaking, if a reaction involves light, heat, and catalytic conversion, it can be regarded as photothermal catalysis. The thermal energy or heat can be produced by photothermal materials (self-heating) or introduced from an external heat source (assisted heating) during the photothermal catalytic process. In this review, we focus on the photothermal catalysis based on the photothermal effect (self-heating), which can modulate the catalytic transformation via the thermochemical or photochemical pathway (Figure 3).[44] In the thermochemical pathway, the photothermal catalytic system can interact with incident light and then dissipate the absorbed photon energy into thermal energy (heat), which can promote the transfer of charge carriers and enhance the catalytic activity. In the photochemical pathway, the photoexcited "hot" carriers (electrons or holes) can be generated under light irradiation and then participate in catalytic reactions.[45] It should be noted that sometimes it is hard to fully differentiate these two intertwined catalytic pathways during a photothermal catalytic process.[44]

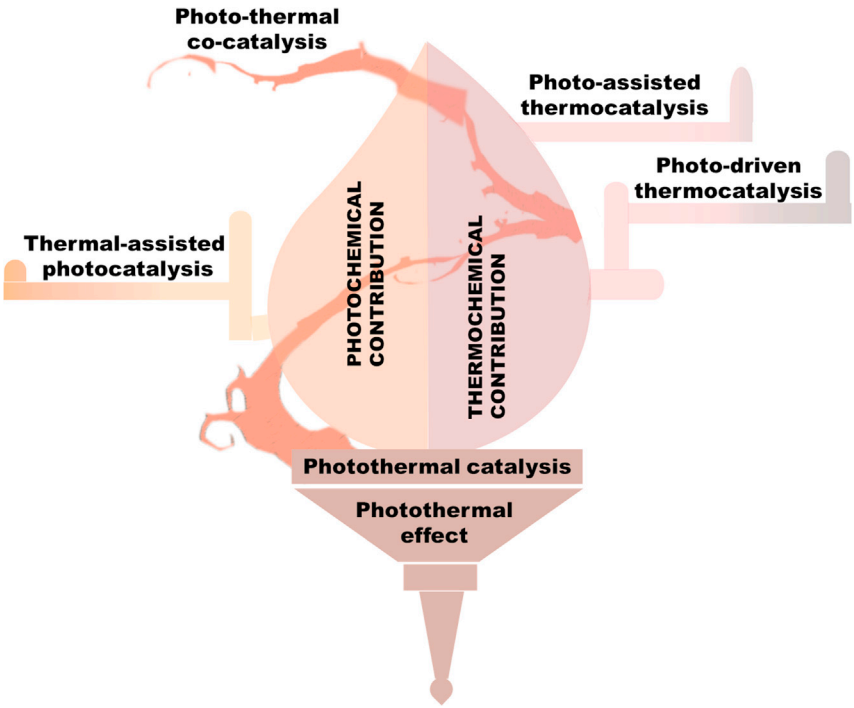

Figure 3. Functioning principles and categories of photothermal catalysis

Under irradiation, hot carriers can be generated in photocatalysts, and their energy is usually much higher than that of carriers generated in thermal excitation. These hot carriers can transfer into unoccupied molecular orbitals of adsorbate molecules and thus induce photochemical transformation, which is completely different from that of traditional thermal pathways. Furthermore, in some cases, it is possible to selectively cause desorption, dissociation, or translational motion of adsorbates on the surface of plasmonic metal nanoparticles by populating specific antibonding resonances of adsorbates.[26] Therefore, one fascinating feature of photothermal catalysis is the possibility of tuning the selectivity toward specific target products via the photochemical pathway in conjugation with the thermal pathway. In other words, some "impossible" chemical reactions and desirable products in thermally driven catalysis can be completed by photothermal catalysis. In addition, heat generation can be localized around active sites resulting from direct local heating in the nanoscale during the photothermal conversion process, avoiding the need for supplying excessive heat to heat up an entire reaction system.[14]

Categories of photothermal catalysis

In photothermal catalysis, light and thermal effects can work separately or collectively. As a result, photothermal catalysis can be classified into three major types of reactions based on their specific reaction pathway(s), i.e., thermochemical or photochemical. The first type is thermal-assisted photocatalytic reaction, in which the main reaction pathway is the photochemical pathway. The catalyst itself cannot enable reactions driven only by heat.[46] The reaction may involve the excited electronic state or hot carriers of photocatalyst. Thermal energy plays an assisting role in further reducing apparent activation energy of photocatalysis, promoting photogenerated carriers' mobility and mass transfer rate, thus accelerating the reaction process (Figure 4A).[47]

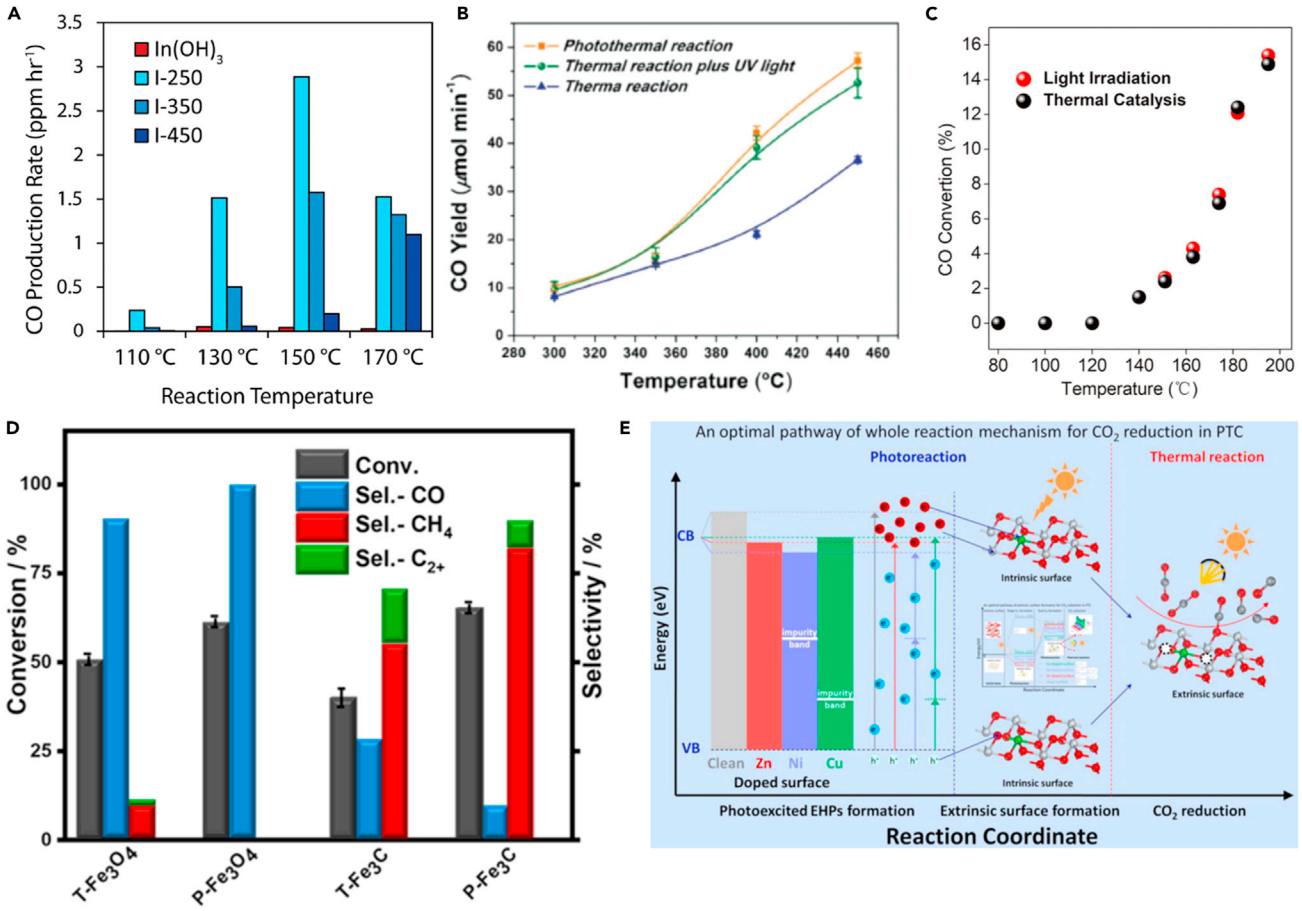

Figure 4. Different types of photothermal catalysis

(A) Thermal-assisted photocatalysis.[47] Copyright 2014 the authors. Published by Wiley-VCH Verlag GmbH & Co. KGaA, Weinheim.

(B) Photoassisted thermocatalysis.[48] Copyright 2016 Wiley-VCH Verlag GmbH & Co. KGaA, Weinheim.

(C) Photodriven thermocatalysis, subtype of (B)[49] Copyright 2018 Wiley-VCH Verlag GmbH & Co. KGaA, Weinheim.

(D) Photothermal co-catalysis.[50] Copyright 2020 American Chemical Society.

(E) Photocatalysis-thermocatalysis cycle (PTC), subtype of (D).[51] EHP, electron-hole pair. Copyright 2017 Elsevier Ltd. All rights reserved.

The second type is photoassisted thermal catalytic reaction, where the main reaction mechanism is the thermochemical pathway, similar to traditional thermal catalysis (Figure 4B).[48] In this case, the reaction involves mainly the ground electronic state of the photocatalyst. Light plays the role of enhancing the local temperature and thus exciting vibrational states via the photothermal effect, with a minor contribution of the photochemical pathway. Thus, proper temperature conditions and good ability to absorb light for the photocatalyst are required for the reaction.[52] The extreme case of this type is photodriven thermocatalysis, where light is utilized only to supply heat. Excellent light absorption ability and light-to-thermal conversion efficiency are needed for this subtype of photocatalyst. The heat generated from solar light is the energy used to increase the temperature of catalysts and reactants, which can avoid the harsh conditions in conventional thermal reactions (Figure 4C).[49]

The third type is photothermal co-catalysis, which is a result of the collective contribution of the thermochemical and photochemical pathways. The heat emitted from the photothermal effect can promote the reaction process through the thermochemical pathway, while the photochemical effect also contributes significantly to the

apparent activity, leading to a synergistic effect of thermal and photochemical pathways that is different from the simple sum of these two pathways[50] (see Figure 4D). The reaction may involve the coupling of the excited electronic states, or hot carriers, with the excited vibrational states (due to thermal energy) of photocatalysts. Sometimes, the synergy between the photocatalytic and the thermocatalytic cycles can occur sequentially. As shown in Figure 4E, in the upper half of the illustrated reaction, oxygen vacancies are produced by UV-visible light (UV-vis) excitation, while in the lower half, CO_2 is thermally catalyzed by oxygen vacancies to CO.[51]

Here are the similarities and differences for all these three types of photothermal catalysis. In terms of similarity, they all absorb solar light as the energy supply to drive a catalytic reaction, while heat is generated from a part of or all the absorbed solar energy. The difference among them is the specific destination (or final forms of energy) of all the absorbed solar energy. In thermal-assisted photocatalytic conversion, the solar energy is primarily used by the photocatalytic pathway, i.e., generating the excited electronic state to induce a reaction, while heat generation is a small part of the absorbed solar energy, e.g., much smaller than the energy used to produce the excited electronic state. In addition, the generated heat will influence the reaction mechanism by exciting vibrations or phonons in the ground electronic state. In contrast, if the photocatalytic pathway is significant in a reaction and the generated heat is a relatively large portion of the absorbed solar energy, photothermal co-catalysis can occur. In this case, the generated heat will influence the reaction mechanism by exciting vibrations or phonons in the excited electronic state, leading to the synergy effect of the thermocatalytic and photocatalytic pathways. For photoassisted thermal catalytic conversion, the absorbed solar energy is mostly used to generate heat, providing excited vibrations or phonons in the ground electronic state. Even though some solar energy can be used to produce excited electronic state via the photochemical pathway, this portion of energy should be much smaller than the energy used to generate the heat for inducing the thermocatalytic pathway.

Consequently, these three types of photothermal catalysis differ in terms of the origin of overall activation energy. In thermal-assisted photocatalysis, the overall activation energy is dominated by the contribution from the photochemical pathway, with some small contribution from the thermochemical pathway. In the photoassisted thermal catalytic reaction, the overall photothermal catalysis is mostly contributed by the thermocatalytic pathway, with only minor contribution from the photothermal pathway. In photothermal co-catalysis, the overall activation energy originates from the comparable contributions of the thermochemical and photochemical pathways, and is usually lower than the simple sum of the activation energies from the thermochemical and photothermal pathways due to the synergy effect.

During photothermal catalysis, sometimes external heat supply (in addition to the heat generated for the photothermal effect of catalysts) may be used to facilitate the reactions, which is practical in terms of applications. The external heat likely will not change the nature (or the type) of a particular photothermal catalysis. From the viewpoint of solar energy utilization, highly efficient photothermal catalysis with less or no external heating supply is desired.

DESIGN OF PHOTOTHERMAL CATALYSTS

Over the past decade, we have witnessed a fast growth in photothermal catalysis,[53–55] and it has demonstrated much higher energy efficiency and catalytic activity than

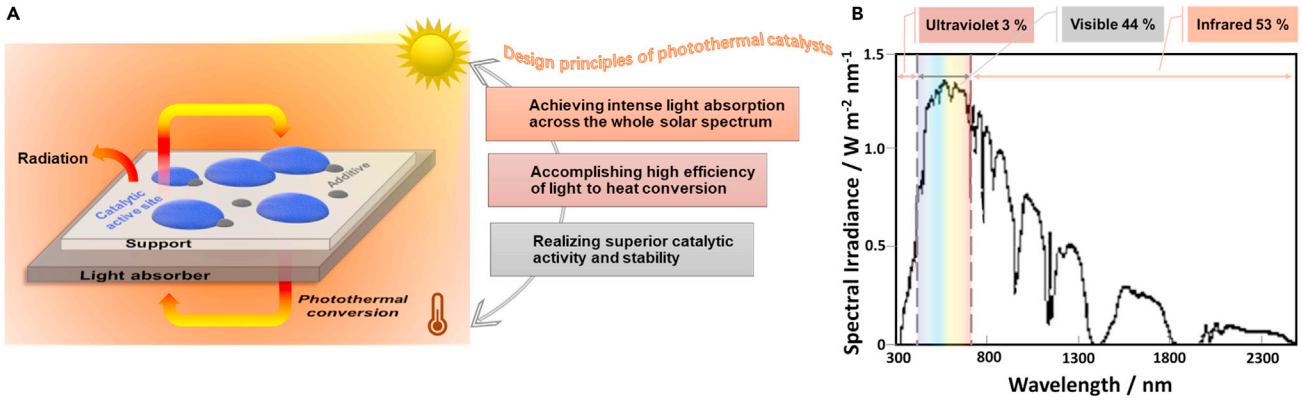

Figure 5. Design of photothermal catalysts.
(A) Schematic diagram of a general photothermal catalyst.
(B) Solar irradiance energy spectrum.

conventional photocatalytic processes or thermocatalytic processes. Actually, the materials and structural engineering at the nanoscale have played crucial roles in the design of good photothermal catalysts.[14] The unique optical and catalytic properties of nanomaterials arise from the size and quantum effects.[56] When the size decreases to the nanometer scale, new properties like tunable effective refractive index, semicontinuous band gap for semiconductors, and local field enhancement effects can be observed. Accordingly, the nanomaterials can enhance the light absorption efficiency and regulate the bandwidth and local field light-heat conversion. Similar size effects have been confirmed in various other heterogeneous catalytic reactions,[57,58] which could determine the product activity or selectivity or even alter the overall catalytic pathway.

Design criteria

Three vital design criteria shall be used for photothermal catalysts to obtain excellent catalytic performance: (1) achieving intense light absorption across the entire solar spectrum, (2) accomplishing high efficiency of light-to-heat conversion, and (3) realizing superior catalytic activity and stability. The first and second criteria mainly depend on the nature and structure of photothermal materials. For the third criterion, it can borrow ideas from the design of traditional thermal and photochemical catalysts.

Based on these three criteria, an effective photothermal catalytic system should possess several important components: light absorber, catalytic support, active sites, and/or co-catalysts (Figure 5A). The light absorber absorbs incident light and effectively converts it to thermal energy (heat) instead of undergoing radiative re-emission, which should be the key component for the performance of photothermal catalysis. Thereby, a good light absorber will exhibit superior optical and thermal properties across the entire solar spectrum (e.g., from 300 to 2,500 nm), with minimal transmittance and reflectance. Then, the produced thermal energy can increase the surface temperature of the catalyst via the heat transfer process. To obtain excellent catalytic performance, sufficient catalytic active sites and an accessible support are two equally important factors in catalyst design, which can determine the activity and stability of photothermal catalysts.[59] Of course, in some cases, the photothermal materials themselves can act as catalytic sites and/or support.[33]

Common photothermal materials

For the design of photothermal catalysts, the crucial factor is to convert light energy to thermal energy maximumly through the design of effective photothermal materials. Hence, in the following section, we will illustrate several typical photothermal materials (or catalysts) in order to guide the catalyst design.

Semiconductors

Semiconductors are widely used in conventional photocatalysis due to their advantages of simple preparation, low cost, and low toxicity with a tunable band gap, while UV light is usually chosen as the irradiation source.[60] However, as shown in Figure 5B, visible (400–760 nm) and IR light (>760 nm) accounts for the majority of the solar light spectrum, as 43% and 53%, respectively, while UV light (290–400 nm) accounts for only 4%. According to $E = h\nu$ (h is the Planck constant, ν means the light frequency), visible and IR light has energy lower than 3.1 eV, which makes it difficult to excite electrons in the valence band for most semiconductors. In other words, UV light is needed as the irradiation source for most semiconductors, which conflicts with the goal to maximize the solar energy utilization efficiency by using the entire solar energy spectrum. Furthermore, the efficiency of photocatalytic processes is extremely low (usually in the range of hundreds of $\mu mol\ g^{-1}\ h^{-1}$), mainly due to the rapid recombination of photogenerated charge carriers in traditional semiconductors with broad band gap.[61] Thus, narrowing the band gap in semiconductors can enhance the light absorption in a wide spectrum and thus facilitate solar-light-induced reactions via the photothermal effect.[62]

Several semiconductors with suitable band gap were revisited owing to the development of photothermal catalysis over the past several years. For instance, semiconductors with a narrow band gap, such as Ti_2O_3[33] nanoparticles, Fe_3O_4,[50] and black titania,[63] have been investigated for photothermal catalysis.

Metallic nanoparticles

Metals are usually excellent conductors of electricity and heat, and can effectively absorb solar energy and convert it into heat. As an important factor that determines the optical properties of metal nanomaterials, the SPR effect can be produced by metallic nanoparticles by a specific irradiation wavelength, leading to strong light absorption. In reported work, it has been demonstrated that the plasmonic metal nanostructures are easy to excite with visible and NIR light, which provides the energy for catalytic reactions via the SPR effect.[64] Indeed, once exposed to light, the catalytic reactions occur on the surface of metallic nanostructures, which can be influenced by the aforementioned three processes involved in SPR. Therefore, enhancing the SPR effect of plasmonic nanomaterials is a way to expand the light absorption spectrum, improve the light-to-heat conversion, and thus enhance the catalytic performance. Currently, plasmonic noble metal photothermal catalysts such as Au, Ag,[65,66] and Ru[67] have received widespread attention. Meanwhile, some non-precious metals, including aluminum (Al),[68] copper (Cu),[69] niobium (Nb),[54] nickel (Ni),[70] and iron (Fe),[50,68,71] have been exploited. The shape, morphology, size, and composition of plasmonic metal nanostructures are the key factors influencing their light-to-heat performance. Govorov and Richardson found that the surface temperature increase of Au nanoparticles was proportional to their size according to numerical simulations.[72] In contrast, it has been reported that the conversion efficiency of light-to-heat decreases when the size of nanoparticles increases, owing to the increased scattering.[73] On the other hand, the previous report demonstrated that the shape and morphology of Au nanoparticles played an important role in

SPR-induced heat generation based on calculation with Green's dyadic method.[74] Nanorods exhibited a pronounced increase in heating efficiency compared with nanospheres. In addition, thin planar structures possessed higher heating efficiency than nanorods.[74]

In addition to the properties of photothermal materials, the photocatalytic performance is decided by the intensity of the incident light. Researchers found that in the early stage of irradiation, the photo-to-thermal conversion efficiency increased quickly as the catalyst bed temperature rose sharply. After that, the conversion efficiency reached a steady state, and further enhancing the illumination intensity caused a decline in efficiency.[50,75]

Despite the richness of variety and controllable morphology in the synthesis of metal nanomaterials, their concerning environmental impact, high cost, and complex preparation process cannot be ignored. Moreover, structural distortion of metal nanoparticles is likely to occur in the presence of acids, alkalis, or salts, and nanoparticles tend to agglomerate under harsh conditions or can be poisoned by trace contamination. These drawbacks restrict their applications.[70]

Carbonaceous materials

Diverse forms of nanocarbon materials (Figure 6), such as biomass-derived amorphous carbon,[76] graphene,[34] graphene oxide (GO) or reduced graphene oxide (rGO),[77] and carbon nanotubes (CNTs),[78] have been reported in photothermal conversion. Owing to their light absorption in a wide range, great stability, high thermal conductivity, and tunable molecular and electronic structures, and the ease of tailoring their micro/macrostructures, carbon nanomaterials have become promising photothermal catalysts. However, it must be noted that the carbon-based materials possess relatively high emissivity (approximately 0.85) due to their high surface reflection. Hence, the surface reflection needs to be reduced in carbon nanomaterials in order to achieve optimal efficient in solar energy conversion.

MOFs

Metal-organic frameworks (MOFs), featuring semiconductor-like behaviors, are connected by metal ion points and supported through organic ligands to complete the formation of 3D extension in space. They have recently attracted significant interest in the fields of photocatalysis and photothermal catalysis.[48] The advantages of regularity, adjustable pore size, diversity of topological structures, and malleability make MOFs a promising type of material for various catalytic reactions, while their controllable band gap is particularly suitable for photocatalysis or photothermal catalysis.

MXenes

Transition metal carbide, carbonatite, and nitride (MXenes) are a new type of 2D materials possessing special electronic and optical characteristics.[83] MXenes can be expressed as $M_{n+1}X_nT_x$ (n = 1–3), where "M" represents the traditional metal, including Sc, Ti, Zr, Hf, V, Nb, Ta, Cr, or Mo; "X" represents carbon or nitrogen; and "T_x" means the surface termination, such as oxygen, hydroxyl, and fluorine. In MXenes, n layers of X are covered by "n + 1" layers of M, arranged in the structure of $[MX]_nM$. $Ti_3C_2T_x$ was the first MXene reported in 2011 for its electronic properties, similar to those of a semiconductor, and outstanding ability in photothermal conversion.[84]

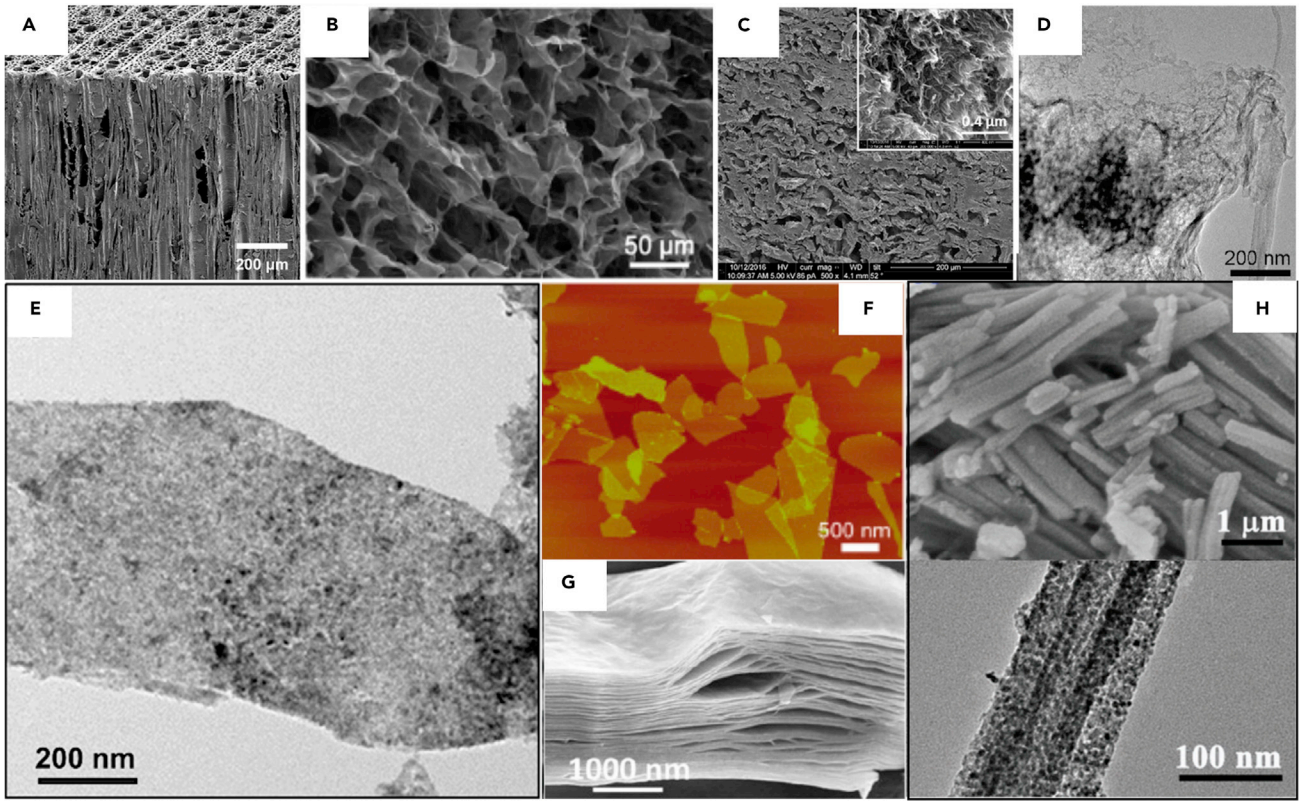

Figure 6. Carbon materials and other photothermal materials

(A) Natural woods.[79] Copyright 2017 Elsevier, Inc.

(B) Graphene oxide (GO).[77] Copyright 2016 Wiley-VCH Verlag GmbH & Co. KGaA, Weinheim.

(C) Functionalized chemically reduced graphene oxide (f-crGO).[34] Copyright 2017 American Chemical Society.

(D) Sulfur-doped graphitic C_3N_4.[80] Copyright 2010 American Chemical Society.

(E) Niobium and titanium carbides (MXenes).[54] Copyright 2021 American Chemical Society.

(F) Functionalized titanium carbide nanosheets.[78] Copyright 2016 Wiley-VCH Verlag GmbH & Co. KGaA, Weinheim.

(G) Two-dimensional ultrathin MXene ceramic nanosheets.[81] Copyright 2016 American Chemical Society.

(H) Surface-passivated beta-Mo_2C nanowires.[82] Copyright 2019 The Royal Society of Chemistry.

Others

In addition to the above-mentioned main types of photothermal materials, other materials such as chalcogenides and polymers (e.g., polypyrrole, polyaniline)[85] can be used as photothermal materials.

Strategies to improve photothermal catalytic performance

The photothermal catalyst needs to absorb solar light as the energy supply to drive a catalytic reaction, while heat is generated from a part of or all the absorbed solar energy. The difference between various photothermal catalysts is the specific destination (or final forms of energy) of all the absorbed solar energy, originating from the differences in their coupling of thermochemical and photochemical pathways. We can apply the knowledge of traditional photocatalysis and thermal catalysis to improve the performance of photothermal catalysts. For instance, if the system temperature of the photothermal catalysis can reach the same level as pure thermal catalysis, the principles for regulating traditional thermal catalysis may be applied to the photothermal catalysis. Similarly, reactions involving photochemical pathways can be tuned by strategies used in traditional photocatalysis. To enhance the photothermal effect and achieve maximum catalytic performance, several common improvement strategies have been developed, including tuning of light absorption,

improvement of heat generation and transfer, and enhancement of catalytic kinetics. Furthermore, another typical and effective approach is to design a composite or multifunctional catalyst that combines the functions of each component to improve the overall catalytic performance.

Tuning of light absorption

From the perspective of solar energy absorption, the visible light region accounts for 44% of the total energy for solar light, and IR light accounts for 53%. Most of the traditional semiconductors absorb only the UV light part (3% of the solar energy).[86] Therefore, how to optimize the sunlight absorption when using semiconductors should be considered when designing photothermal catalysts. A common design strategy is to modify the semiconductor catalyst via the introduction of defects or vacancies, which can adjust the physical and chemical properties of semiconductors.[87,88] The defect structures can broaden the light absorption range and accelerate the separation rate of photogenerated carriers. For example, the cost-effective Bi_2O_{3-x} with oxygen vacancies exhibited strong absorption in the wavelength range of 600–1,400 nm due to the SPR effect (Figures 7A–7C), demonstrating efficient photoconversion of CO_2 to CO even under NIR light irradiation with low intensity.[89]

Apart from tuning the light absorption ability of the material, another efficient way to enhance photocatalysis performance is to transform unused red and NIR radiation into available UV-vis light by up-conversion of luminescent materials. For example, P. Esparza et al. found improvement of commercial TiO_2 in the photocatalytic decomposition of methylene blue in water.[92] G. Liu et al. proved the promotion of up-conversion agents in solar water-splitting efficiency for hematite (α-Fe_2O_3).[93]

Similarly, for carbon-based materials, a facile strategy is to increase refraction and scattering inside the materials through the construction of nanostructures,[94,95] such as hierarchical graphene foam,[94] in which sunlight can be trapped and subsequently absorbed through multiple internal reflections.[95] Meanwhile, the light-shielding effect of graphene sheets is a significant obstacle for their application in photocatalytic areas, mainly due to their unavoidable exposure to light. In addition to controlling the dosage of these graphene sheets to relieve the negative effects of light shielding, structure regulation, such as using small or in-plane holey materials composited with semiconductors, is feasible as well.[96]

For plasmonic metal nanostructures, the optical properties are adjustable by their size, shape, and composition. Thus, the rational design of plasmonic nanostructures with optimal size, shape, and composition is the way to increase the conversion efficiency of solar energy. In addition, the plasmonic band can be tuned from the visible to the NIR region using hollow structures, such as nanocages or nanoframes.[97] The nanostructures with broad plasmonic bands in the visible and NIR regions is an ideal platform to investigate photothermal catalysis.

In general, the light absorption ability of catalysts is very important for light-driven reactions; therefore, tuning of light absorption is applicable to all kinds of photothermal catalysts.

Improvement of heat generation and transfer

From the viewpoint of energy transfer, the conversion of light to heat and the following heat transfer are crucial for photothermal catalysis. And then, improvement of heat generation and transfer is a potential method to improve photothermal catalytic performance, especially for materials with low light-to-heat conversion

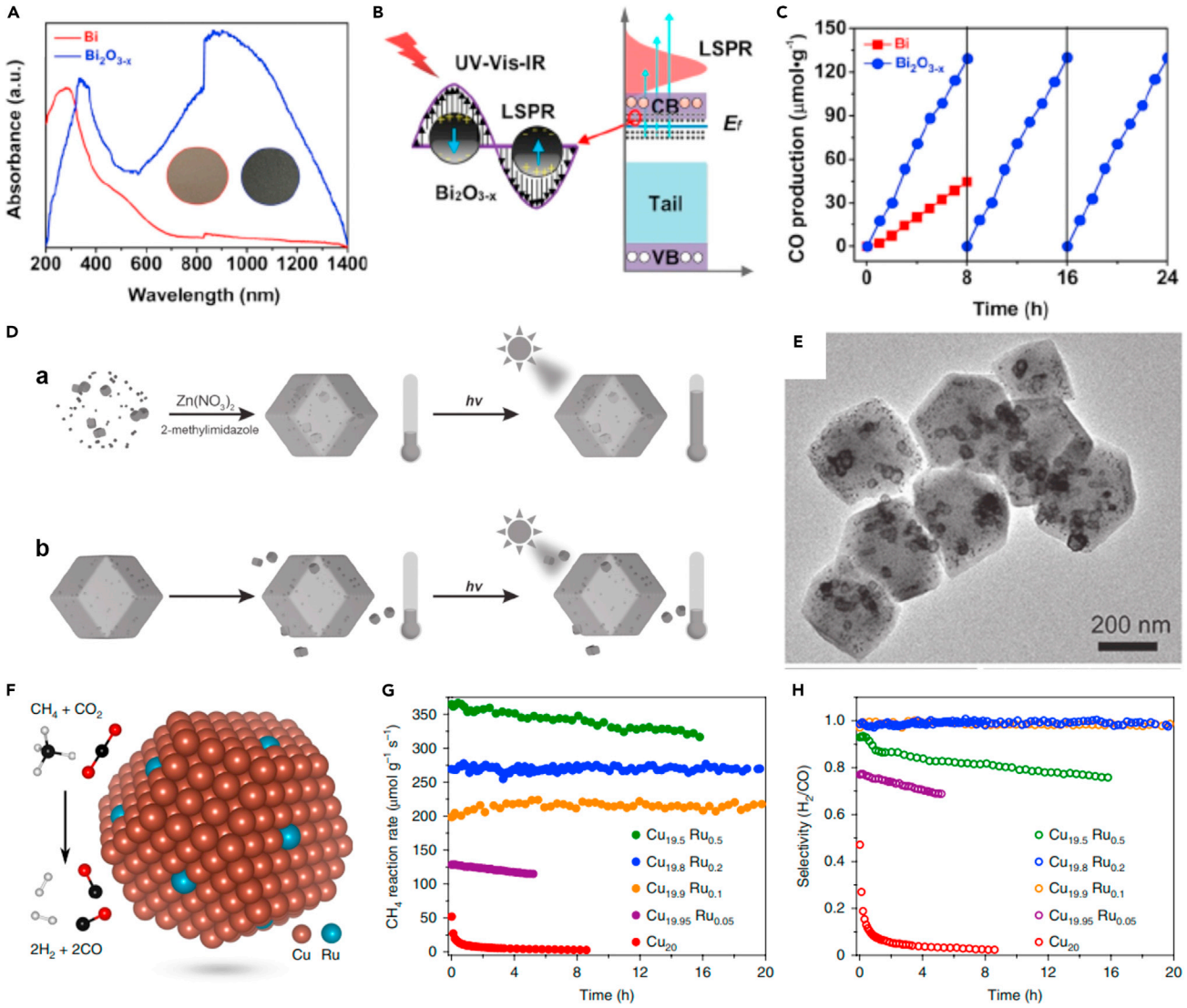

Figure 7. Effective strategies to improve catalyst performance

(A–C) Plasmonic hot electrons from oxygen vacancies for infrared light-driven catalytic CO_2 reduction on Bi_2O_{3-x}.[89] Copyright 2020 Wiley-VCH GmbH.
(A) UV-vis-IR absorption spectra (inset: photos of Bi [left] and Bi_2O_{3-x} [right]).
(B) Schematic illustration of LSPR excitation on Bi_2O_{3-x}. (C) The cycling test for photocatalytic CO production over Bi_2O_{3-x}.
(D and E) Integration of photothermal effect and heat insulation to efficiently reduce reaction temperature of CO_2 hydrogenation.[90] Copyright 2016 Wiley-VCH Verlag GmbH & Co. KGaA, Weinheim. (D) Schematic illustration of the formation and the temperature variation under light irradiation of (a) Au&Pt@ZIF and (b) Pt@ZIF + Au. The dots represent the Pt nanocubes, while the cubes represent the Au nanocages. (E) Transmission electron microscopy images of Au&Pt@ZIF.
(F–H) Light-driven methane dry re-forming with single atomic site antenna-reactor plasmonic photocatalysts.[91] Copyright 2020 the authors, under exclusive license to Springer Nature Ltd. (F) Schematic of a Cu-single-atom Ru surface alloy catalyst with the dry re-forming reactants and products shown on the left. (G and H) Reaction rate (G) and long-term stability (H).

efficiency. After the electronic excitation by photons, the photonic energy should be converted into thermal energy effectively, rather than being reflected or radiatively re-emitted. Meanwhile, heat utilization has important impacts on the catalytic performance. Actually, the surface temperature of photothermal catalysts is usually higher than that of the surrounding environment due to localized heating. To enhance reaction activity, it is necessary to maximize the heat transfer efficiency from the catalysts to the reactants absorbed on their surfaces. Therefore,

photothermal catalysts with large specific surface area, high thermal conductivity, and strong reactant adsorption capacity are favorable for photothermal catalysis. In this case, the heat energy is utilized to drive the catalytic reaction, instead of being lost to the surroundings via convection and conduction.[17,95] An alternative idea is to cover the catalysts with a thermal insulation layer to prevent or reduce heat loss.[98] For instance, a zeolite imidazolate framework (ZIF-8) can be used to encapsulate plasmonic metal nanoparticles to form a hybrid structure (Figures 7D and 7E), where ZIF-8 can act as an "insulator" to inhibit heat loss.[90]

Enhancement of catalytic kinetics

For heterogeneous catalysis, it is well known that the activation of reactant molecules occurs on the active sites of catalytic surfaces.[99] Hence, increasing the number of active sites is an effective way to enhance the photothermal catalytic activity. In particular, increasing active sites could greatly improve the catalytic efficiency for catalysts that already have excellent light-to-heat conversion capabilities. For example, it was reported by Henderson et al. that photoexcited hot carriers, coupled with single-atom active sites, could improve the catalytic activity toward dry re-forming of CH_4 (Figures 7F–7H).[91] Theoretical calculations using quantum chemistry modeling indicated that single-atom doping of Ru on the Cu (111) surface, combined with excited-state activation, resulted in a substantial reduction in the energy barrier for CH_4 activation. Synthesizing supported materials like metal oxides is an essential way to provide the adsorption and activation sites for reactants at interfaces by constructing strong interactions between reactants and metal support. Introduction of co-catalyst or active noble metals such as Pt, Pd, and Ru[100] is another way to improve the photothermal catalytic activity.

Formation of hybrid nanostructures

The construction of hybrid nanostructures is a popular and straightforward strategy to enhance photothermal catalytic performance. In this way, the catalytic activity can be synergistically improved via the integration of two or more components into the hybrid photothermal catalysts. Usually, these photothermal catalysts consist of plasmonic or non-plasmonic metallic nanoparticles loaded on the inorganic support (mainly metal oxides), in which a different role can be played by each component. The following are common hybrid nanostructures in photothermal catalysis.

Metal/semiconductor structures

Introduction of metal nanoparticles such as Pt, Au, or Ag[101] as a co-catalyst can alleviate some of the intrinsic issues of semiconductor photocatalysts. These co-catalyst nanoparticles can extend the lifetime of photoinduced charge carriers and improve the separation rate of electron-hole pairs at the interface of the metal/semiconductor. However, for most semiconductors, this approach still faces several issues, including poor absorption of low-energy photons, short photon penetration depth, and short diffusion length of charge carries.[101] Combination of plasmonic metals and semiconductors can effectively address these issues by using the SPR effect. In the plasmonic metal/semiconductor nanostructures, the plasmonic nanoparticles can interact with light in a wide range of the solar energy spectrum, especially visible light, and thus dramatically enhance the generation and transfer of hot electrons. Meanwhile, it can modify the band gap of semiconductors via the formation of a Schottky barrier at the interface, and thus trap the transferred hot electrons.[44,101] A typical nanostructure of this framework is Au/TiO_2.[102] It was reported that the deposition of Au nanoparticles onto the rutile can enhance the visible light harvest and improve the production yields of CO and CH_4 under a wide solar energy

spectrum owing to the SPR of Au nanoparticles and the direct heat generation from IR light.[103]

Non-plasmonic transition metals such as Pt, Pd, Ir, and Rh loaded on semiconductors can exhibit the photothermal effect via the interband or intraband transition of photoexcited electrons. According to the work from Zhu's group,[104] the bound electrons in non-plasmonic transition metals can be excited (under light with short wavelengths) to a high-energy band via the interband electronic transitions, and the excited electrons with sufficiently high energy can transfer to the LUMO of adsorbed reactant molecules on the surface of metal nanoparticles, similar to the photoexcited electrons in plasmonic metal nanoparticles. The electrons excited by the low-energy visible or IR light also enhance reaction rates via the photothermal effect. These electrons do not have enough energy to be injected into adsorbate states. Obviously, the non-plasmonic metals/semiconductors are promising photothermal catalysts, as non-plasmonic metal nanoparticles are widely employed for important organic chemical synthesis in traditional thermal catalysis.

Metal/MOF or semiconductor/MOF hybrid structures

MOFs have been widely used in various thermal catalytic reactions due to their high porosity and high surface area. According to the literature, the photothermal effect of MOFs can be determined by the optical absorption of the MOF.[105] However, the photothermal catalysts based on MOFs have not been widely investigated owing to their relatively weak absorption in the visible and IR regions. To improve the catalytic efficiency, a common strategy is to integrate plasmonic metal nanoparticles or plasmonic semiconductor materials with MOFs, which can harvest visible or NIR light owing to their wide-range tunable LSPR band.[44]

In a recent report, the Pd nanocube (NC)@ZIF-8 composite was fabricated through the encapsulation of Pd nanocubes into ZIF-8, exhibiting superior catalytic activity toward selective catalytic hydrogenation of olefins under irradiation.[106] The Pd nanocube cores effectively convert light into heat via plasmonic photothermal effects, while the ZIF-8 shell protects the Pd cores, accelerates the catalytic hydrogenation via H_2 enrichment, and facilitates substrate selection with a specific size for selective catalysis. Subsequently, this group designed composites of Pt nanocrystals/porphyrinic MOFs (PCN-224), which exhibited remarkable catalytic activity in aromatic alcohol oxidation under light owing to the synergy between the photothermal effect and the generation of singlet oxygen.[107] A hybrid nanostructure of core-shell Cu_7S_4@ZIF-8 was reported for a valuable cyclocondensation reaction under laser irradiation. The core of Cu_7S_4 hollow microspheres served as a nano-heater due to the NIR plasmonic photothermal effect, and the catalytic shell of ZIF-8 showed enhanced activity for the cyclocondensation reaction.[108]

CHARACTERIZATION OF PHOTOTHERMAL CATALYSIS

Characterization of photothermal catalysts is very important for understanding the catalytic mechanism and thus for the catalyst design. Most characterization methods for traditional thermal catalysis and photocatalysis can be applied to photothermal catalysis. Typically, the chemical composition of catalysts can be analyzed through the elemental composition (inductively coupled plasma [ICP], energy-dispersive X-ray [EDX], electron energy-loss spectrum [EELS], high-angle annular dark-field [HAADF] imaging) or the chemical state and structure (X-ray diffraction [XRD], X-ray photoelectron spectroscopy [XPS], X-ray adsorption spectroscopy [XAS], Fourier transform infrared [FTIR] spectroscopy, Raman). The physical properties and

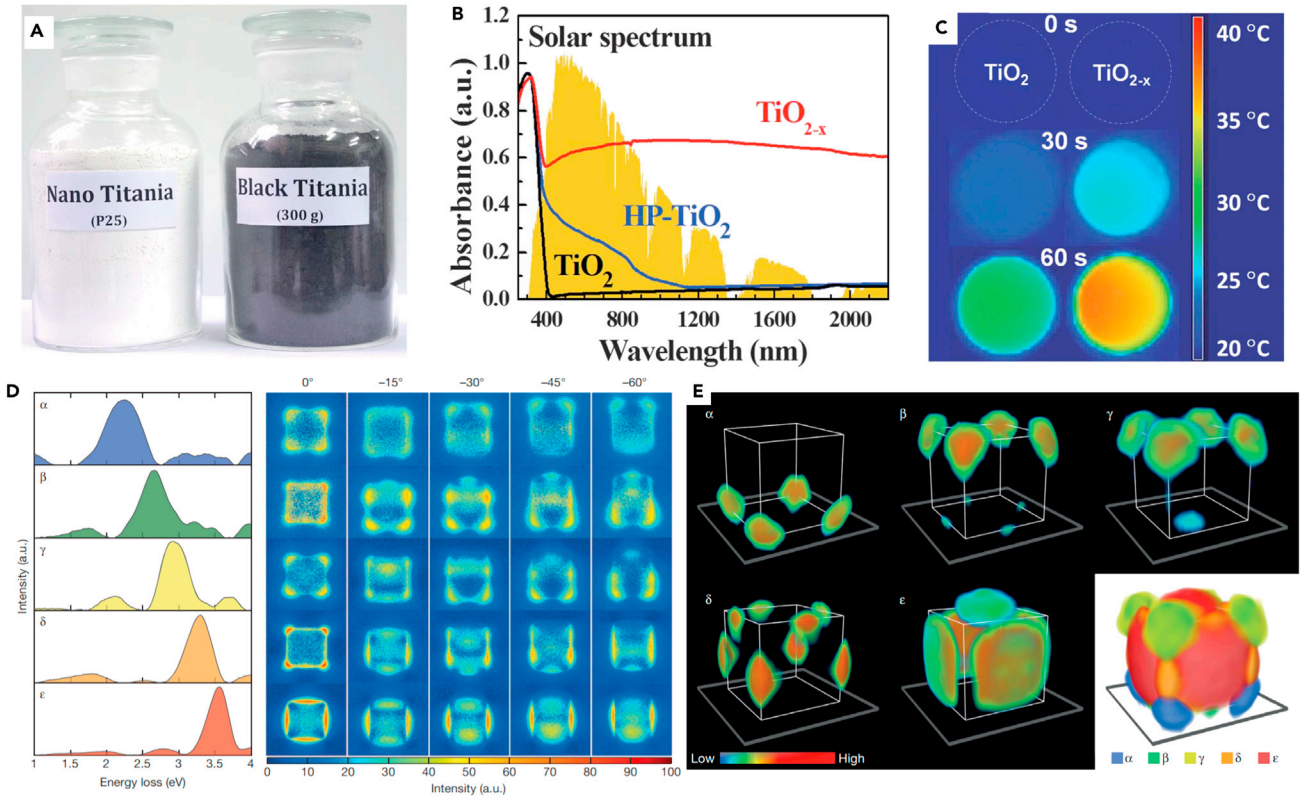

Figure 8. Characterization of photothermal catalysis

(A–C) Visible-light photocatalytic, photoelectrochemical, and solar thermal properties of aluminum-reduced black titania.[110] Copyright 2013 The Royal Society of Chemistry. (A) Mass production of black titania (TiO_{2-x}) using the Al-reduction method. (B) Absorption spectra of the 500°C-reduced TiO_{2-x} sample, the high-pressure-hydrogenated black titania (HP-TiO_2), and pristine titania (TiO_2). (C) Thermal image map of cool-pressed disks (from TiO_2 and 500°C-reduced TiO_{2-x} powders) after irradiation under an AM 1.5G Xe lamp solar simulator for different times.

(D and E) Three-dimensional imaging of localized surface plasmon resonance of metal nanoparticles.[111] Copyright 2013 Macmillan Publishers Ltd.

(D) EELS maps of LSPR components of a silver nanocube.

(E) Three-dimensional visualization of the LSPR components of a silver nanocube. Copyright 2013 Springer Nature.

nanostructure of catalysts can be observed by electron microscopy (SEM, transmission electron microscopy [TEM], high-resolution TEM [HR-TEM], atomic force microscopy [AFM]). Gas adsorption-desorption analysis[109] (gas ad) is often utilized to test the ability of catalysts to adsorb species in thermal catalysis. The defects can be confirmed by electron spin resonance (ESR) or XPS. The thermal stability of catalysts can be measured with thermal gravimetric analysis (TGA). The electronic band structure plays a major role in deciding the optical absorption ability of a semiconductor. Therefore, it is necessary to characterize the band structure in photocatalysis (density functional theory [DFT], UV photoelectron spectroscopy [UPS], XPS). All of the above characterization methods can be applied to photothermal catalysis.

Ex situ characterization and computational methods of photothermal catalysis

For the photothermal catalytic systems, the characterizations of light absorption and photothermal conversion ability are very important, such as the methods of UV-vis-NIR spectrometry and IR camera. For example, the absorption spectra and thermal image maps of black titania can be resolved through the UV-vis spectra and IR camera, respectively (Figures 8A–8C).[110] In addition, the 3D images related to LSPRs can be reconstructed through EELS. For example, 3D images of a single silver nanocube were obtained via the analysis of EELS maps (Figures 8D and 8E).[111] The LSPR

spectral components (α–ε) resulting from non-negative matrix factorization (NMF) to the spectrum images at different tilt angles are shown in Figure 8D, and the normalized EELS maps corresponding to five NMF components are shown on the left. A tomographic reconstruction of the EELS maps related to the respective LSPR components displays a combined 3D rendering of all the components (Figure 8E). These techniques enable an in-depth understanding of photothermal mechanisms.

Apart from conventional characterization methods, theoretical chemistry calculations and computational simulations, such as finite-difference time-domain (FDTD) simulations[112] and DFT,[44] could be adopted to understand the interaction of light with catalysts and the photothermal effect in the photothermal catalytic process. The FDTD and discrete dipole approximation (DDA) calculations can be used to simulate the field distributions and cross sections of plasmonic metal nanostructures under incident light. DFT, a common theoretical method in thermocatalysis, can be employed to investigate the electronic structures and adsorbed species and intermediates on the surface of catalysts and illustrate the reaction pathways during photothermal catalysis. Ye and colleagues investigated the catalytic mechanism of a Rh/TiO_2 catalyst for CH_4 activation.[113] The results from DFT calculations indicated that photoexcited hot electrons in Rh 4d orbitals can transfer to unoccupied 3d orbitals in Ti, resulting in the formation of electron-deficient sites ($Rh^{\delta+}$) on the surface. These sites of $Rh^{\delta+}$ can accept electrons from CH_4, thereby promoting CH_4 activation through cleavage of C–H bonds. Ma et al. used DFT calculations to illustrate the difference in reaction pathways of CO_2 conversion for two photothermal catalysts: Fe_3C and Fe_3O_4.[50]

In situ and *operando* characterization of photothermal catalysis

Recently, *in situ* and *operando* (operating or working) characterizations have been developed for the study of heterogeneous catalysis due to its unique features, including spectroscopic,[114] scattering, and microscopic techniques,[115] as well as the application of synchrotron radiation[116] sources to improve the spatial and temporal resolution. *In situ* characterization focuses on the study of a catalyst under model or true reaction conditions, and the *operando* characterization involves simultaneous study of a catalyst and its performance during an actual reaction.[117] During the photothermal catalytic process, *in situ* measurements not only correlate the characterization results of a photothermal catalyst with its catalytic performance, but also reveal new phenomena attributed to its accuracy and practicality. Many *in situ* and *operando* characterizations applied in photocatalysis or thermocatalysis (Figure 9) can be extended to photothermal catalysis, including gas ad, ESR, FTIR, Raman, XAS, XPS, XRD, TEM, and SEM, which can take exemplary benefits such as monitoring the change of properties and studying the catalytic mechanism, especially photochemical pathways.

In our previous work, a series of Fe-based catalysts was prepared through a simple hydrogenation/carbonization treatment with commercial Fe_3O_4 as a precursor, exhibiting tunable selectivity of hydrocarbons and CO in photothermal CO_2 conversion.[50] The stability of Fe-based catalysts was studied by *in situ* XAS (Figures 10A and 10B). Moreover, using the evidence from transient absorption (TA) spectroscopy (Figures 10C and 10D) and *in situ* time-resolved diffuse reflectance IR Fourier transform spectroscopy (DRIFTS) (Figures 10E and 10H), the photothermal catalytic mechanisms were investigated to understand non-thermal effects and selectivity difference of the Fe-based catalysts toward CO_2 photoconversion.

The photoinduced charge separation and transfer are crucial for determining the activity under irradiation or photothermal conditions, but most conventional

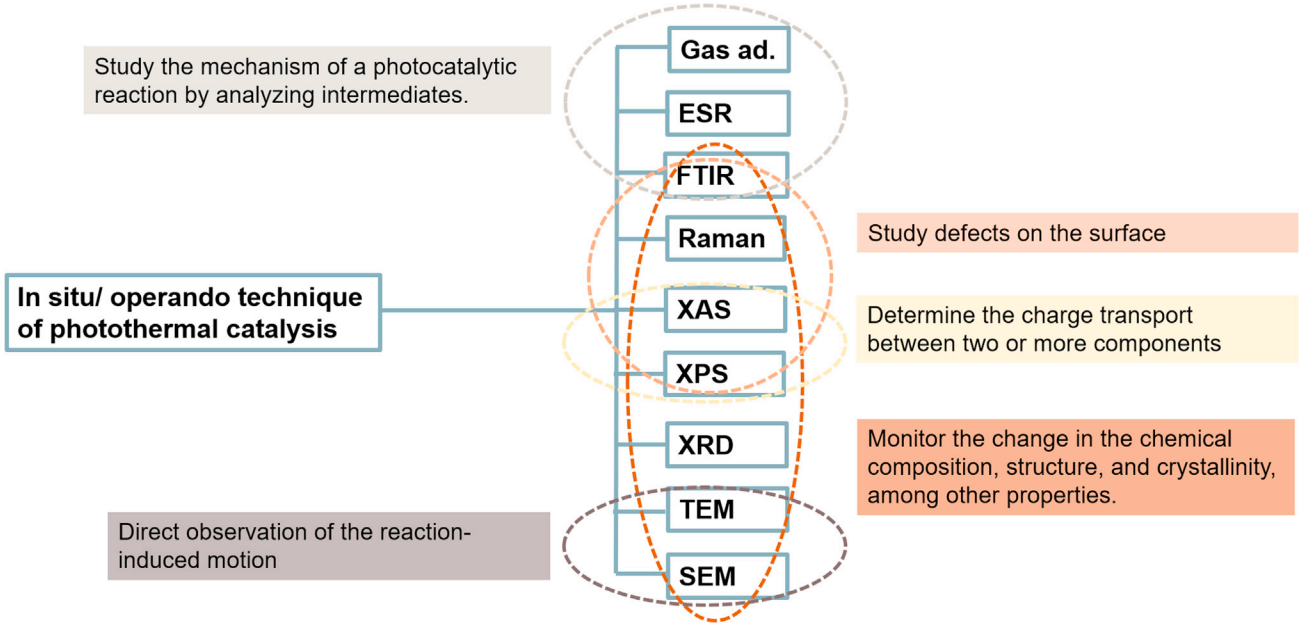

Figure 9. *In situ/operando* characterization of some important properties of photothermal catalysis

Nomenclature and abbreviations: gas ad., gas adsorption-desorption analysis; ESR, electron spin resonance; FTIR, Fourier transform infrared spectroscopy; XAS, X-ray absorption spectroscopy; XPS, X-ray photoelectron spectroscopy; XRD, X-ray diffraction; TEM, transmission electron microscopy; SEM, scanning electron microscopy.

characterizations could not provide sufficient information about these assignments. Alternatively, an *in situ* irradiation X-ray photoelectron spectroscopy (SI-XPS) technique to explore the interfacial interactions as well as charge transfer has been applied to light-induced heterogeneous catalysis. Tang et al. found the superior activity of iron species dispersed on titanium dioxide toward methane oxidation to methanol with high selectivity under ambient conditions.[118] Through SI-XPS, it was found that iron species work as electron acceptors, as the Fe 2p binding energy increases with lamp on, while electrons excited from the valence band (oxygen 2p orbitals) of TiO_2 jump to the conduction band and then (titanium 3d orbits) transfer to the iron species during the CH_4 conversion process. Bi and co-workers utilized SI-XPS to directly observe the dynamic interfacial bonding and charge transfer in metal-free (black phosphorus/covalent triazine framework [BP/CTF]) photocatalysts for efficient hydrogen evolution.[119] These SI-XPS results clearly revealed photogenerated electrons efficiently transferred from CTF to BP surfaces through their interfacial P–C bonds under light excitation, which significantly promoted photocatalytic activity and stability for the hydrogen evolution reaction (HER). Interestingly, when the light irradiation was turned off, all the typical peaks of both BP and CTF were returned back to their original state, indicating that the electron transfer between CTF and BP is a reversible process. These *in situ* methods significantly assist the understanding of fundamental mechanisms during the photo-involved catalysis process.

PHOTOTHERMAL APPLICATION IN HETEROGENEOUS CATALYSIS

As a new type of catalytic process, other than thermocatalysis and photocatalysis, the seminal work on photothermal catalysis can be dated back to 1998, when Kennedy and Datye first reported the synergistic effect of photothermal heterogeneous oxidation of ethanol over Pt/TiO_2.[120] In 2014, Ye and colleagues designed a series of nanocatalysts based on group VIII metals (Ru, Rh, Ni, Co, Pd, Pt, Ir, and Fe),

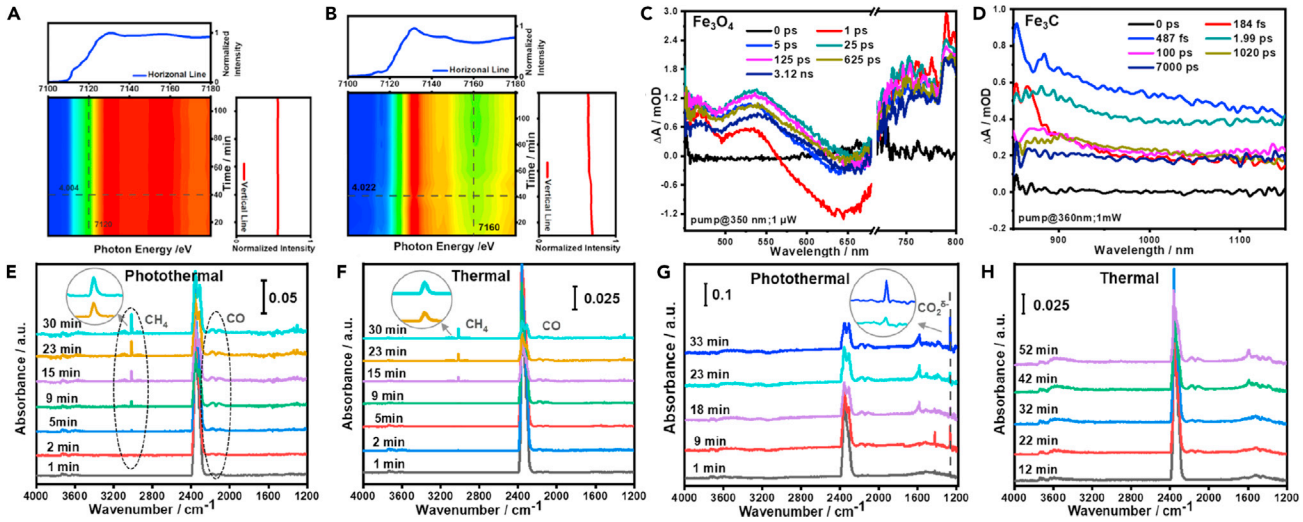

Figure 10. ***In situ/operando*** **characterization of photothermal conversion of CO_2**

(A and B) *In situ* XAS spectra of (A) Fe_3C and (B) Fe_3O_4.

(C) Ultrafast TA spectra of Fe_3O_4 probed at indicated delays pumped by a 350 nm pulse.

(D) Ultrafast TA spectra of Fe_3C probed at indicated delays pumped by a 360 nm pulse.

(E) *In situ* time-resolved DRIFTS spectra of Fe_3C under irradiation.

(F) *In situ* time-resolved DRIFTS spectra of Fe_3C under the thermal condition (at 310°C).

(G) *In situ* time-resolved DRIFTS spectra of Fe_3O_4 under irradiation.

(H) *In situ* time-resolved DRIFTS spectra of Fe_3O_4 under the thermal condition (at 350°C).[50] Copyright 2020 American Chemical Society.

expanding the use of the photothermal effect for the catalytic conversion of CO_2 (with H_2) into CH_4 (Sabatier reaction) and CO (reverse water-gas shift reaction).[121] A compelling photothermal CO_2 reaction rate (mol h^{-1} g^{-1}) was achieved, much higher than that of the photocatalytic reaction (μmol h^{-1} g^{-1}). Meanwhile, the photothermal methanation of CO_2 over Ru nanoparticles on black silicon nanowire (Si-NW) supports was reported by Ozin and co-workers.[67] These works demonstrated a new catalytic pathway for the photoconversion of CO_2. To date, various photothermal catalytic applications have been developed for the production of solar fuels and chemicals (Figures 11A and 11B). In the following section, we will discuss several typical photothermal catalytic processes for producing fuels and chemicals.

Water splitting

Water splitting via the photothermal catalytic process can resolve the problem of energy loss or sluggish reaction kinetics of traditional photocatalysis or electrocatalysis. Recently, it was reported that the HER can be enhanced by single-atom silver-incorporated g-C_3N_4 (SAAg-g-C_3N_4),[123] exhibiting superior activity and stability in photocatalytic HER (PER) and solar-heat-assisted HER processes. The catalytic improvement of SAAg-g-CN can be ascribed to available Gibbs free energy of the adsorbed hydrogen atom (ΔG_{H^*}) and the formation of N–Ag bonding. When the temperature increased from 25°C to 55°C, the PER rate rose dramatically, implying the conductive influence of heat in the catalytic reaction. Furthermore, some systems of assembling three fields, including thermal, photo-, and electrocatalysis, for water splitting were reported.[124] In 2019, Zhang and colleagues presented a photothermal-effect-driven strategy to promote the electrocatalytic HER and oxygen evolution reaction (OER) activities of nickel/rGO bifunctional electrocatalysts, demonstrating that a photothermal effect induced by Ni/rGO could greatly improve catalytic performance due to facilitation of the thermodynamics and kinetics of

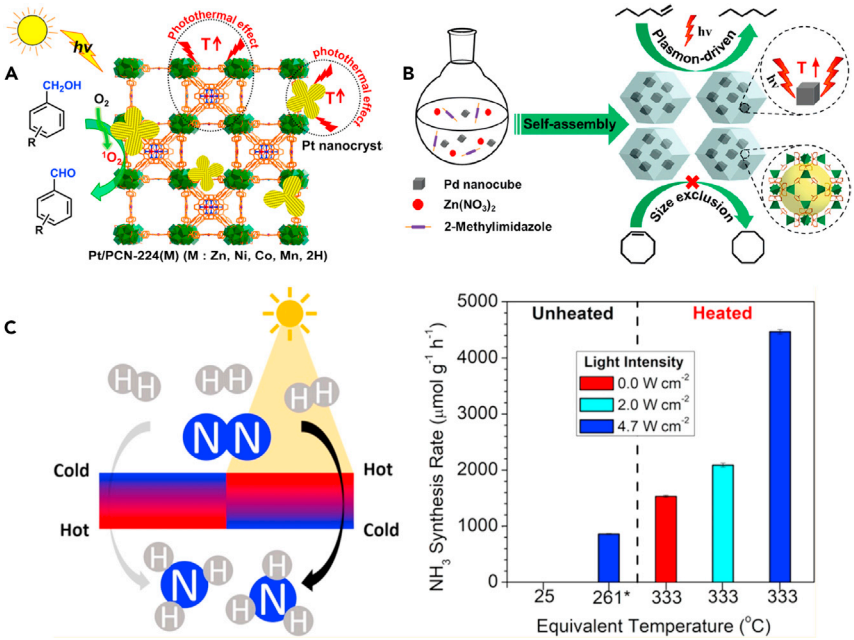

Figure 11. Application of photothermal effect in heterogeneous catalytic reaction systems

(A) Schematic illustration showing the singlet-oxygen-engaged selective oxidation of alcohols over Pt/PCN-224(M) using molecular oxygen under visible-light irradiation.[107] Copyright 2017 American Chemical Society.

(B) Self-assembly of Pd NCs@ZIF-8 and plasmon-driven selective catalysis of the hydrogenation of olefins.[106] Copyright 2016 Wiley-VCH Verlag GmbH & Co. KGaA, Weinheim.

(C) Light-induced thermal gradients in ruthenium catalysts significantly enhance ammonia production.[122] Copyright 2019 American Chemical Society.

electrocatalysis.[125] Zhou et al. studied the catalytic activity of a bifunctional Ni nanosheet array integrated thermoelectric (TE) device.[126] It acted as a photothermal conversion layer and thermoelectric generator integrated with efficient HER, thus exhibiting an excellent overall water-splitting performance.

Synthesis and decomposition of NH_3

The surface of catalysts could be quickly raised to 300°C–500°C with good photothermal materials, which would greatly enhance catalytic activity in gas-solid phase reactions.[50,121] More importantly, the photothermal effect is able to supply sufficient heat energy for thermodynamically unfavorable reactions even under mild conditions, thus avoiding harsh reaction conditions (e.g., high temperature and high pressure). The energy-intensive Haber-Bosch process for ammonia synthesis has been pursued for both high reaction rates and high yields during the past decades.[127] These conflicting objectives require a complex balance of optimized catalysts, suitable temperatures, high pressures, and multiple recycling steps. A breakthrough design pathway was reached recently. In 2019, Liu et al. reported a Ru-based catalyst produced ammonia with high reaction rates and conversion yields under light.[122] Ammonia can be copiously produced under continuous-wave light-emitting diodes that simulate concentrated solar illumination, instead of external heating or elevated pressures. As shown in Figure 11C, this work confirmed that thermal gradients created and controlled by photothermal heating of catalyst surfaces were responsible for the high reaction rates and yields. In addition, the non-thermal plasmonic effects were eliminated. As a reverse route, ammonia decomposition is crucial for pollutant removal from water, air, and soil, while it does not require much energy

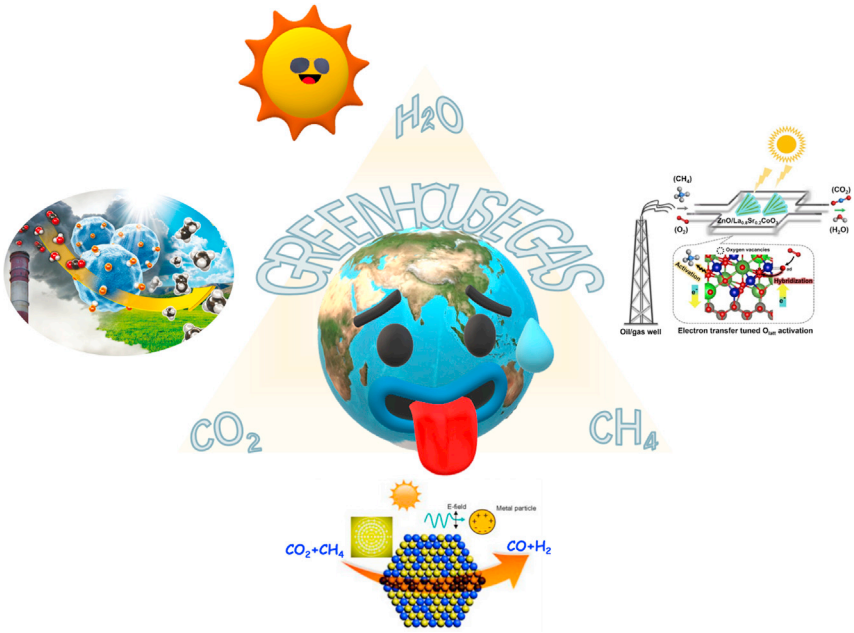

Figure 12. Solar-driven photothermal catalytic conversion of greenhouse gases[131–133]

input to occur under photothermal conditions. Long and co-workers prepared ultrafine TiO_2 encapsulated in a nitrogen-doped porous carbon framework to decompose ammonia gas under irradiation, showing compelling activity with 100% ammonia decomposition in a light irradiation of 5 min.[128] The excellent performance can be attributed to the specific structure and high efficiency of light absorption, as well as the accelerated separation of photoinduced carriers.

Conversion of C_1 molecules

C_1 molecules, including CO_2, CH_4, and CO, as abundant and cheap carbon sources, can be converted into fuels and various high-value-added chemicals, and this can be regarded as the fundamental catalytic process for the modern chemical industry related to coal and natural gas. More importantly, the emission of greenhouse gases (mainly CO_2 and CH_4) causes global warming and environmental damage. Hence, the transformation of C_1 molecules has been one of most active research fields in heterogeneous catalysis in the past decades[129] (Figure 12). However, the activation and conversion of C_1 molecules are very difficult due to the inert nature of C–H in CH_4 and the C–O bond in CO_2 and the uncontrollable coupling of C–C bonds. Therefore, it is impressive to convert C_1 molecules to valuable feedstock or fuels via photothermal catalysis without high energy consumption and harsh reaction conditions.[68,130]

CO_2 and CO conversion

The 3d transition metals, such as Fe, Co, Ni, Ru, Rh, and Pt,[67,71,113] are usually used as solar-driven catalysts for C=O activation. Compared with precious metals, the non-precious metals, including Fe, Co, and Ni, are promising for CO and CO_2 conversion due to their low cost and facile preparation in large quantities.

In our previous work, we reported a solar-driven Fischer-Tropsch reaction to olefin (FTO) process using Fe_5C_2 nanoparticles (Figures 13A–13D). The Fe_5C_2 nanoparticles exhibited highly efficient utilization of light and excellent photothermal

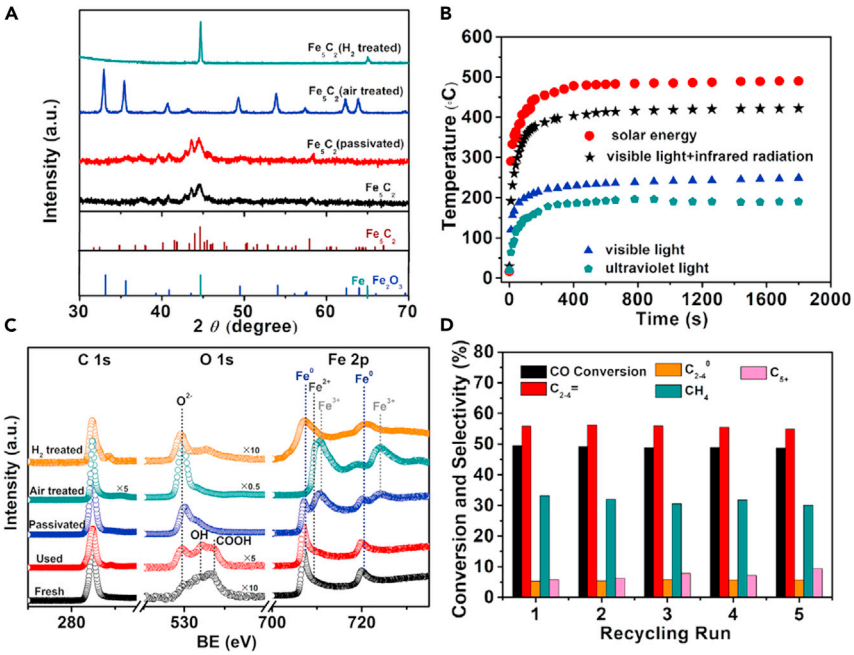

Figure 13. Fe_5C_2 catalyst characterization and reaction performance of CO hydrogenation

(A) XRD patterns of Fe_5C_2 and reference catalysts.

(B) Monitoring of the catalyst bed temperature of Fe_5C_2 catalyst under photoirradiation.

(C) *Ex situ* XPS spectra of Fe_5C_2 catalyst at different treatment conditions.

(D) Recycling of the Fe_5C_2 catalyst for five cycles. Reaction conditions: no external heating, catalyst mass 180 mg, CO/H_2 1/2, irradiation time 0.5 h, 300 W Xe lamp. After each reaction, new reactants were added and a new reaction began.[75] Copyright 2018 Elsevier, Inc.

performance, resulting in an olefin/paraffin (o/p) ratio of 10.9 and low CO_2 selectivity (18.9%), with CO conversion of 49% (Figure 13). In contrast, the thermally driven catalytic process provided a dominant product of CH_4 with high selectivity of 95.1% in hydrocarbons and CO_2 (36.0% of all products) and a negligible o/p ratio (0.1).[75] The surface of the Fe_5C_2 catalyst was partly decorated by oxygen atoms under irradiation (see Figure 13C), which can modify the local electronic structure and the optical band gap of the surface, leading to easy C_2H_4 desorption, overhydrogenation to C_2H_6, and thus a high selectivity to olefins. This work reported a high-performance, energy-efficient, and green FTO process with solar as the energy source and cost-effective iron carbide as the catalyst, which shows the potential of using solar energy in the production of industrially important chemicals. Recently, we found a tunable selectivity in photothermal CO_2 conversion over a series of Fe-based catalysts developed through a simple hydrogenation/carbonization treatment with commercial Fe_3O_4.[50] The selectivity toward hydrocarbon (CH_x) can be modulated by the extent of hydrogenation/carbonization of the Fe_3O_4 precursor. Among them, Fe_3O_4 produced almost pure CO, while the obtained Fe_3C displayed very high selectivity toward hydrocarbons under the photothermal conditions. This work provided an example of the construction and preparation of low-cost and efficient Fe-based catalysts with tunable selectivity of products to CO_2 conversion. Similarly, Zhang et al. reported a process of CO_2 hydrogenation to C_{2+} alkanes via a photothermal process. A series of novel CoFe-based catalysts was successfully fabricated by hydrogen reduction of CoFeAl layered-double-hydroxide (LDH) nanosheets at 300°C–700°C (Figure 14).[68] With increasing LDH-nanosheet reduction temperature, the CoFe-x catalysts showed a progressive selectivity shift from CO to CH_4, and eventually to high-value hydrocarbons (C_{2+}), and the CoFe-650 catalyst showed remarkable

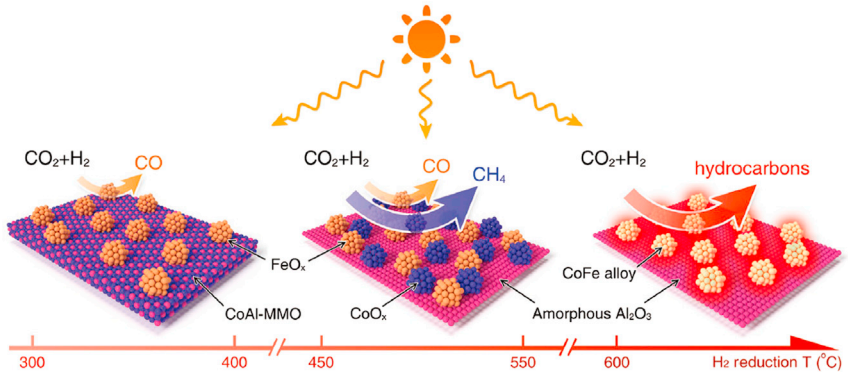

Figure 14. Illustration of different CoFe-x catalysts formed by hydrogen reduction of a CoFeAl-LDH nanosheet precursor at different temperatures[68]

selectivity toward hydrocarbons (60% CH_4, 35% C_{2+}). Their results demonstrate a vibrant new catalyst platform for harnessing clean and abundant solar energy to produce valuable chemicals and fuels from CO_2.

Another idea for photothermal conversion of CO_2 is to combine the H_2 produced from water splitting. Grimes and co-workers reported that reduced blue titania sensitized with bimetallic Cu-Pt nanoparticles generated a substantial amount of both methane and ethane by CO_2 photoreduction under simulated sunlight (Figure 15A).[131] Over a 6 h period, 3.0 mmol g^{-1} methane and 0.15 mmol g^{-1} ethane were obtained, while no H_2 nor CO was detected, whereas the isotopic tracer experiments confirmed that the hydrocarbon products originated from CO_2 and water (Figures 15B–15E).

CH_4 activation

CH_4 is composed of one carbon and four hydrogen atoms through sp^3 hybridization, forming a very stable tetrahedron structure. There are several methods to convert methane, including methane coupling, methane oxidation, methane dry re-forming, and steam re-forming,[113,134,135] which usually need high temperatures for C–H bond activation in thermal catalysis. Miyauchi et al. demonstrated the enhancement of oxidation of methane (POM) to produce syngas under UV irradiation using noble metals (Rh, Pd, Ru, and Pt) incorporated in a molecular sieve.[136] Guo et al. reported a solar-driven efficient methane oxidation process under high-velocity continuous flow over the $ZnO/La_{0.8}Sr_{0.2}CoO_3$ (ZnO/LSCO) heterojunctions.[132] Meanwhile, Zhang et al. reported photoassisted thermal catalytic methane combustion over $PdO/Mn_3O_4/CeO_2$ nanocomposites supported on 1D halloysite nanotubes.[52] It was confirmed that strong synergistic effects among components can reduce the methane light-off temperature to below 180°C under irradiation. The increased concentration of Ce^{3+} should be attributed to the promoted ability of absorbing and activating oxygen, thus ensuring the fast and stable redox equilibrium of PdO → Pd → PdO during the catalysis. For dry re-forming reactions, Ye et al. designed PdAu alloy plasmonic nanoparticles, exhibiting enhanced catalytic performance in a methane dry re-forming reaction under visible light.[133] Recently, Ding and colleagues reported the photothermal synergetic CO_2 conversion with CH_4 over NiCo alloys derived from AlMg hydrotalcite, demonstrating a high light-to-fuel efficiency and a low carbon deposition rate.[70] The excellent activity can be attributed to the high solar absorptance of NiCo alloys and the photoenhanced

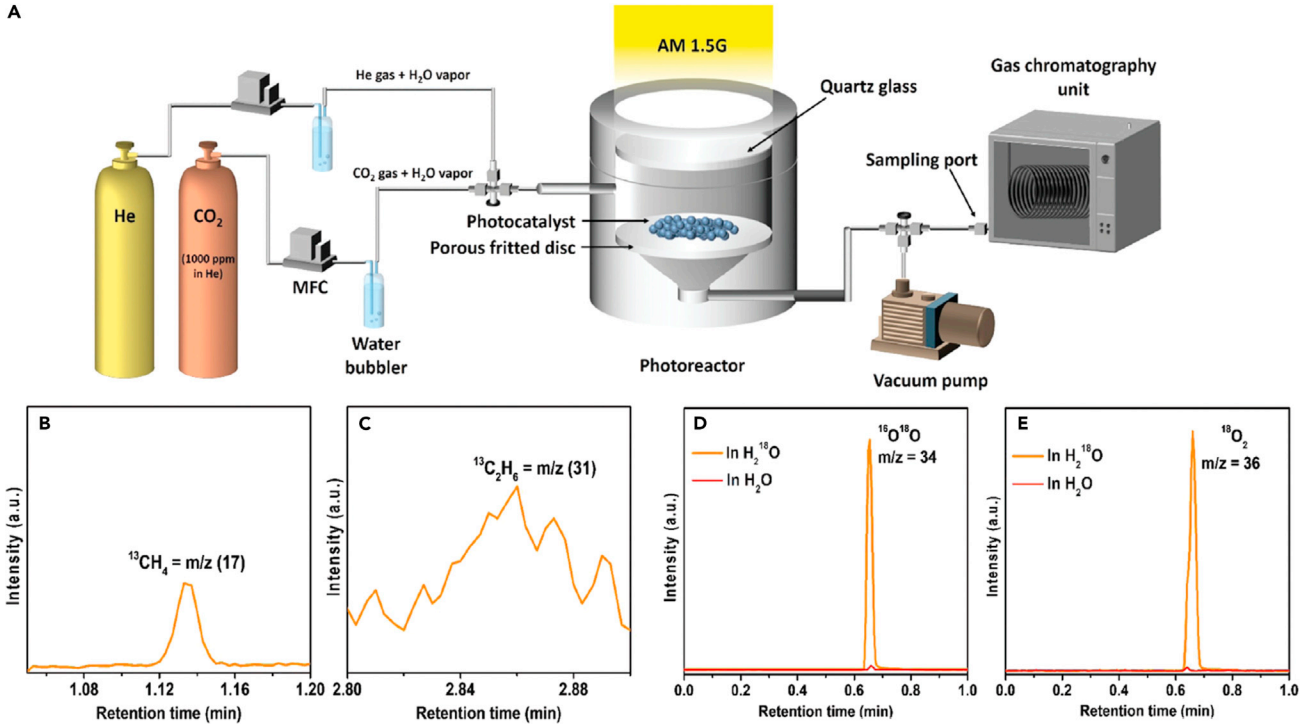

Figure 15. Photothermal conversion of CO_2 and water to hydrocarbon fuels

(A) Schematic illustration of the setup used for CO_2 to fuel photoreduction experiments.

(B–E) Gas chromatography-mass spectrometry (GC-MS) results. Isotopic $^{13}CH_4$ (B), isotopic $^{13}C_2H_6$ (C), $^{16}O^{18}O$ (D), and isotopic $^{18}O_2$ (E) generated over $Cu_{1.00\%}$-$Pt_{0.35\%}$-BT.

With respect to sample identification, BT denotes blue titania, Cu and Pt concentrations are given in wt %; $Cu_{x\%}$-$Pt_{y\%}$-BT indicates that Pt was deposited upon BT with subsequent deposition of Cu.[131] Copyright 2019 The Royal Society of Chemistry.

reactant activation, while the stability benefited from the reduced energy barriers of CH* oxidation to CHO* and increased energy barriers of CH* dissociation to C*, indicated by DFT calculations. However, the product of photothermal catalytic CH_4 was mainly CO. Despite the progress, photothermal conversion of CH_4 to high-value hydrocarbons remains a significant challenge.

Other reactions

Photothermal catalysis can be used in other hydrogenation and oxidation reactions, including the conversion of organics,[137] pollution degradation,[138] and medical treatments.[21] The photothermal heterogeneous oxidation of ethanol can be observed over Pt/TiO_2.[120] The photothermal synergistic enhancement of CO_2 production was found due to gas-phase transport of intermediates between the two catalyst phases in a mixed serial-parallel kinetic pathway. The Pt/PCN-224(Zn) composite combines the advantages of both Pt nanocubes and PCN-224(Zn), exhibiting excellent catalytic activity and selectivity in the oxidation of primary alcohols to aldehydes based on their photothermal effect and singlet oxygen production ability (Figure 11A).[107] Recently, Fang and co-workers found that KA oil (cyclohexanol and cyclohexanone) can be produced in high selectivity from cyclohexane photothermal oxidation using graphene oxide coupled with Ag and Fe_3O_4 nanoparticle composites under mild conditions. However, less than 50% selectivity to KA oil was obtained under thermal conditions higher than 140°C.[139] Jia and colleagues reported that the degradation of toluene can be improved with a Pt nanoparticle-MnO catalyst under photothermal conditions,

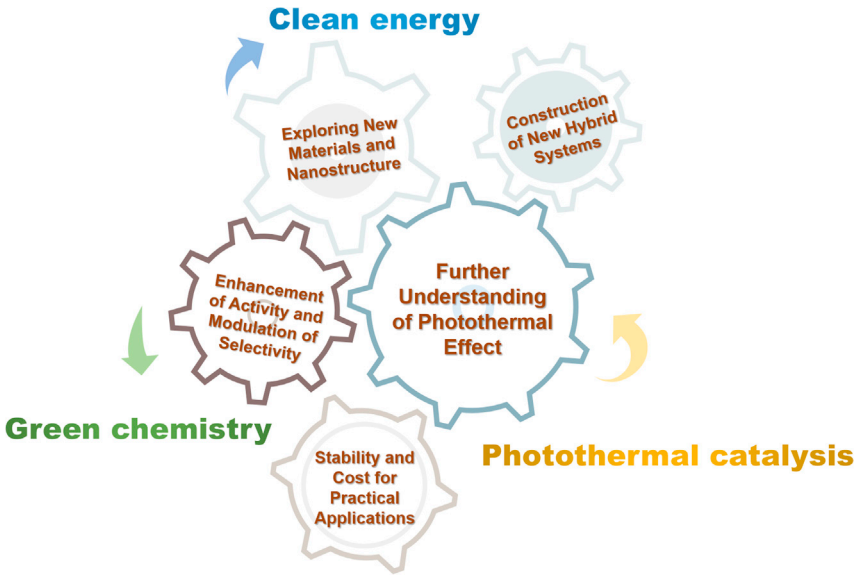

Figure 16. Possible schemes for future development and application of photothermal catalysis

confirming that illumination can not only supply thermal energy to trigger the reaction of toluene oxidation, but also further evoke more lattice oxygen on Pt/MO to participate in toluene decomposition.[140]

SUMMARY AND OUTLOOK

In this review, we have introduced the functioning principles of photothermal catalysis based on different mechanisms of photothermal effects. The synergy of thermochemical and photochemical contributions underlying the photothermal effect is the main cause driving the catalytic reactions for photothermal catalysis, leading to significant enhancement of catalytic performance compared with traditional thermocatalysis and photocatalysis. To provide in-depth understanding of photocatalysis, three types of photothermal catalysis are categorized based on their specific coupling modes of thermal and photochemical pathways. A comprehensive analysis of the different photothermal materials based on their photothermal mechanisms is the key for designing a photothermal catalytic process. Three design criteria and four major strategies are illustrated for photothermal catalyst design. Many characterizations can be extended to the photothermal catalytic systems, especially *in situ* and *operando* characterizations, facilitating discernment of the dominant pathway between photochemical contribution and thermal effect. As an emerging research field, photothermal catalysis has exhibited great potential to drive a wide variety of catalytic reactions under mild conditions without high energy inputs, including water splitting, NH_3 synthesis/decomposition, and conversion of C_1 molecules (CO, CO_2, and CH_4). Hence, we hope to share our perspective on the opportunities for and challenges to the development and application of photothermal catalysis (Figure 16) in the future.

Exploring new materials and nanostructure

During the past decades, we have witnessed enormous progress in new photothermal materials for the utilization and conversion of solar energy. For example, a high level, above 90%, of solar evaporation efficiency has been reported under ambient solar flux with effective photothermal materials.[14,17] We anticipate that new

materials, such as MOFs and 2D nanostructured materials, will further improve photothermal catalytic performance in the future. Actually, 2D nanostructured materials, mainly including Xenes (e.g., arsenene, antimonene, borophene, phosphorene, tellurene) and binary-enes (MXenes and transition-metal dichalcogenide), have attracted extensive interest due to their unique morphology and properties since the discovery of 2D carbon-graphene.[141] For instance, 2D BP with different layers can hold a tunable band gap (from 0.3 to 2 eV), covering the regions of visible light to far IR light in the solar spectrum. These photothermal materials can be further exploited as light absorbers and/or active sites for the design of effective photothermal catalysts. In addition, for different reactions, due to different conditions and mechanisms, the targeted design of new materials and nanostructures is necessary. The type of active center, size effect, and shape-selective catalysis should be considered when designing the catalyst, which can be learned from the experiences of thermal catalysis and photocatalysis.

In addition, the nanostructure of catalysts would be another important factor for the construction of photothermal catalysts that can have great impact on the absorption of light, heat generation and transfer, and mass transfer of reactant and product, and thus determine the catalytic performance. Knowledge from the design and engineering of nanostructures in nanotechnology, such as mesoporous, hollow, or 3D foam nanostructures, could powerfully impel photothermal catalysis to a high development level in the next years.

Construction of new hybrid systems

Hybrid structures or systems would be a facile strategy to enhance photothermal catalytic performance owing to their inherent features and functions. Each component can maximumly perform its own function through the design of materials and structures in the hybrid photothermal catalysts, and thus significantly enhance photothermal catalytic performance. One of the most studied hybrid systems is that of plasmonic metals/semiconductors, demonstrating noteworthy catalytic activity. Taking advantage of new photothermal materials, various hybrid systems exhibiting high photothermal efficiency and superior catalytic activity would be developed, such as core-shell plasmonic metals/MOFs and metals/COFs, hybrid structures of plasmonic metals/BP, semiconductors/MXenes, and plasmonic metals/semiconductors/MXenes. In addition, photothermal systems consisting of inorganic or polymer hosts as light absorber functionalized by homogeneous molecular catalysts would be promising, although they are rarely reported so far.[142]

In-depth understanding of the photothermal effect

Despite the fact that recent achievements in photothermal catalysis have been demonstrated, further understanding is needed to optimize the photothermal catalytic processes. More importantly, it will be pivotal to understand the photothermal effect and discern the catalytic mechanism, including the relaxation and transfer of hot carriers at the femtosecond timescale. As the destination of utilized solar energy varies in different types of photothermal catalysts, it will be a key research question in the future to figure out the exact distribution of different forms of energy conversion (e.g., from light to heat, or light to electronic excited states) in a photothermal catalysis. Characterization techniques, such as *in situ* and *operando* measurements, should be employed to discern the catalytic mechanism under light in the future. Of course, it is a big challenge to combine light into these characterization processes without any negative side effects. In addition, developing new theoretical and computational methods, such as quantum chemistry-based reaction kinetics models and time-dependent chemical models, would be an efficient way to elucidate photothermal mechanisms.

Enhancement of activity and modulation of selectivity

Although great advancements in photothermal catalysis have been presented here, tremendous work is still needed to enhance catalytic activity, owing to the obvious gap between current progress and the requirements of industrial applications. On the other hand, xenon lamps and LEDs are usually used as light sources instead of natural sunlight in most of the reported work. Obviously, the actual catalytic activity with photothermal catalysts under sunlight would be much lower than that under lab conditions due to the lower intensity of sunlight. In addition, another useful method for enhancing activity is to improve the reaction devices, which can concentrate sunlight to a small area, thereby increasing the local optical density.

During photothermal catalysis, the selectivity of desirable products can be modulated by controlling the reaction pathways, which is very challenging and attractive for the conversion of C_1 molecules. Moreover, the available incident light wavelength or light intensity can increase the selectivity of expected products. Of course, further fundamental understanding will be needed to modulate the selectivity of products and catalytic pathways via reliable characterization techniques under *in situ* or *operando* conditions.

Stability and cost of practical applications

As a new arena different from traditional thermocatalysis, photothermal catalysis should achieve superior catalysis stability for long-term operations in large scale as well as satisfactory conversion and product selectivity. Indeed, mild reaction conditions in photothermal catalysis can possess obvious advantages in terms of stability and recyclability of catalysts, and also provide distinct benefits in terms of sustainability. Hence, long-term stability of photothermal catalysts needs to be further explored. It must be pointed out that the deactivation mechanism of catalysts under light has been rarely investigated, and this would give useful guidelines for developing effective photothermal catalysts. Characterization techniques, such as *in situ* and *operando* spectroscopy, can be used to ascertain the deactivation process of catalysts under light. Although excellent catalytic performance can be obtained with noble-metal-based (e.g., Au, Ag, Pd, Pt, Ru, Rh, and Ir) photocatalysts, high cost and scarcity would present significant obstacles to large-scale applications of these catalysts. Developing abundant and low-cost photothermal catalysts, such as Fe- and Ni-based catalysts, chalcogenides, nitrides, and pnictogenides, would be a potential avenue. For the new photothermal materials, such as MOFs and MXenes, the preparation procedures, cost, and intrinsic stability still face many challenges, which may have a long way to go for practical applications.

ACKNOWLEDGMENTS

This work was financially supported by the National Natural Science Foundation of China (21725301, 21932002, 21821004, and 21872104) and the National Key R&D Program of China (2017YFB0602200). Z.Y. is grateful for support from the Natural Science Foundation of Tianjin for Distinguished Young Scholar (20JCJQJC00150). D.X. acknowledges support from the endowed Jacob F. Buckman Chair fund. D.M. acknowledges support from the Tencent Foundation through the XPLORER PRIZE.

AUTHOR CONTRIBUTIONS

Z.Y., D.X., and D.M. proposed the topic of the review and supervised the manuscript. C.Q.S. and Z.H.W. wrote and revised the manuscript. All authors contributed to discussions and manuscript review.

REFERENCES

1. Jiao, F., Li, J., Pan, X., Xiao, J., Li, H., Ma, H., Wei, M., Pan, Y., Zhou, Z., Li, M., et al. (2016). Selective conversion of syngas to light olefins. Science *351*, 1065–1068.

2. Wang, J., Kattel, S., Hawxhurst, C.J., Lee, J.H., Tackett, B.M., Chang, K., Rui, N., Liu, C.-J., and Chen, J.G. (2019). Enhancing activity and reducing cost for electrochemical reduction of CO_2 by supporting palladium on metal carbides. Angew. Chem. Int. Ed. *58*, 6271–6275.

3. Ritchie, H., and Roser, M. (2020). "Energy" Published Online at OurWorldInData.Org. https://ourworldindata.org/energy.

4. Shih, C.F., Zhang, T., Li, J., and Bai, C. (2018). Powering the future with liquid sunshine. Joule *2*, 1925–1949.

5. Chu, S., and Majumdar, A. (2012). Opportunities and challenges for a sustainable energy future. Nature *488*, 294–303.

6. Zhao, Y., Gao, W., Li, S., Williams, G.R., Mahadi, A.H., and Ma, D. (2019). Solar-versus thermal-driven catalysis for energy conversion. Joule *3*, 920–937.

7. Koepf, E., Alxneit, I., Wieckert, C., and Meier, A. (2017). A review of high temperature solar driven reactor technology: 25 years of experience in research and development at the Paul Scherrer Institute. Appl. Energ. *188*, 620–651.

8. Elimelech, M., and Phillip, W.A. (2011). The future of seawater desalination: energy, technology, and the environment. Science *333*, 712–717.

9. Ni, G., Li, G., Boriskina, S.V., Li, H., Yang, W., Zhang, T., and Chen, G. (2016). Steam generation under one sun enabled by a floating structure with thermal concentration. Nat. Energy *1*, 16126.

10. Boddy, P.J. (1968). Oxygen evolution on semiconducting TiO_2. J. Electrochem. Soc. *115*, 199.

11. Fujishima, A., and Honda, K. (1972). Electrochemical photolysis of water at a semiconductor electrode. Nature *238*, 37–38.

12. Sastre, F., Puga, A.V., Liu, L., Corma, A., and García, H. (2014). Complete photocatalytic reduction of CO_2 to methane by H_2 under solar light irradiation. J. Am. Chem. Soc. *136*, 6798–6801.

13. Ghoussoub, M., Xia, M., Duchesne, P.N., Segal, D., and Ozin, G. (2019). Principles of photothermal gas-phase heterogeneous CO_2 catalysis. Energy Environ. Sci. *12*, 1122–1142.

14. Zhu, L., Gao, M., Peh, C.K.N., and Ho, G.W. (2018). Solar-driven photothermal nanostructured materials designs and prerequisites for evaporation and catalysis applications. Mater. Horiz. *5*, 323–343.

15. Dong, S., Zhao, Y., Yang, J., Liu, X., Li, W., Zhang, L., Wu, Y., Sun, J., Feng, J., and Zhu, Y. (2021). Visible-light responsive PDI/rGO composite film for the photothermal catalytic degradation of antibiotic wastewater and interfacial water evaporation. Appl. Catal. B *291*, 120127.

16. Sau, T.K., Rogach, A.L., Jäckel, F., Klar, T.A., and Feldmann, J. (2010). Properties and applications of colloidal nonspherical noble metal nanoparticles. Adv. Mater. *22*, 1805–1825.

17. Gao, M., Zhu, L., Peh, C.K., and Ho, G.W. (2019). Solar absorber material and system designs for photothermal water vaporization towards clean water and energy production. Energy Environ. Sci. *12*, 841–864.

18. Zhu, L., Gao, M., Peh, C.K.N., Wang, X., and Ho, G.W. (2018). Self-contained monolithic carbon sponges for solar-driven interfacial water evaporation distillation and electricity generation. Adv. Energy Mater. *8*, 1702149.

19. Gao, M., Peh, C.K., Zhu, L., Yilmaz, G., and Ho, G.W. (2020). Photothermal catalytic gel featuring spectral and thermal management for parallel freshwater and hydrogen production. Adv. Energy Mater. *10*, 2000925.

20. Robinson, J.T., Tabakman, S.M., Liang, Y., Wang, H., Sanchez Casalongue, H., Vinh, D., and Dai, H. (2011). Ultrasmall reduced graphene oxide with high near-infrared absorbance for photothermal therapy. J. Am. Chem. Soc. *133*, 6825–6831.

21. Yin, Z., Zhang, W., Fu, Q., Yue, H., Wei, W., Tang, P., Li, W., Li, W., Lin, L., Ma, G., et al. (2014). Construction of stable chainlike Au nanostructures via silica coating and exploration for potential photothermal therapy. Small *10*, 3619–3624.

22. Mishra, A., and Bäuerle, P. (2012). Small molecule organic semiconductors on the move: promises for future solar energy technology. Angew. Chem. Int. Ed. *51*, 2020–2067.

23. Chen, C., Kuang, Y., and Hu, L. (2019). Challenges and opportunities for solar evaporation. Joule *3*, 683–718.

24. Jiang, N., Zhuo, X., and Wang, J. (2018). Active plasmonics: principles, structures, and applications. Chem. Rev. *118*, 3054–3099.

25. Seh, Z.W., Liu, S., Low, M., Zhang, S.-Y., Liu, Z., Mlayah, A., and Han, M.-Y. (2012). Janus Au-TiO_2 photocatalysts with strong localization of plasmonic near-fields for efficient visible-light hydrogen generation. Adv. Mater. *24*, 2310–2314.

26. Brongersma, M.L., Halas, N.J., and Nordlander, P. (2015). Plasmon-induced hot carrier science and technology. Nat. Nanotechnol. *10*, 25–34.

27. Aslam, U., Rao, V.G., Chavez, S., and Linic, S. (2018). Catalytic conversion of solar to chemical energy on plasmonic metal nanostructures. Nat. Catal. *1*, 656–665.

28. Zhou, L., Tan, Y., Wang, J., Xu, W., Yuan, Y., Cai, W., Zhu, S., and Zhu, J. (2016). 3D self-assembly of aluminium nanoparticles for plasmon-enhanced solar desalination. Nat. Photon. *10*, 393–398.

29. Zhu, M., Li, Y., Chen, F., Zhu, X., Dai, J., Li, Y., Yang, Z., Yan, X., Song, J., Wang, Y., et al. (2018). Plasmonic wood for high-efficiency solar steam generation. Adv. Energy Mater. *8*, 1701028.

30. Link, S., and El-Sayed, M.A. (1999). Size and temperature dependence of the plasmon absorption of colloidal gold nanoparticles. J. Phys. Chem. B *103*, 4212–4217.

31. Jain, P.K., Lee, K.S., El-Sayed, I.H., and El-Sayed, M.A. (2006). Calculated absorption and scattering properties of gold nanoparticles of different size, shape, and composition:applications in biological imaging and biomedicine. J. .Phys .Chem. B *110*, 7238–7248.

32. Link, S., Wang, Z.L., and El-Sayed, M.A. (1999). Alloy formation of gold-silver nanoparticles and the dependence of the plasmon absorption on their composition. J. Phys. Chem. B *103*, 3529–3533.

33. Wang, J., Li, Y., Deng, L., Wei, N., Weng, Y., Dong, S., Qi, D., Qiu, J., Chen, X., and Wu, T. (2017). High-performance photothermal conversion of narrow-bandgap Ti_2O_3 nanoparticles. Adv. Mater. *29*, 1603730.

34. Yang, J., Pang, Y., Huang, W., Shaw, S.K., Schiffbauer, J., Pillers, M.A., Mu, X., Luo, S., Zhang, T., Huang, Y., et al. (2017). Functionalized graphene enables highly efficient solar thermal steam generation. ACS Nano *11*, 5510–5518.

35. Chen, Q., Pei, Z., Xu, Y., Li, Z., Yang, Y., Wei, Y., and Ji, Y. (2018). A durable monolithic polymer foam for efficient solar steam generation. Chem. Sci. *9*, 623–628.

36. Fan, Q., Wu, L., Liang, Y., Xu, Z., Li, Y., Wang, J., Lund, P.D., Zeng, M., and Wang, W. (2021). The role of micro-nano pores in interfacial solar evaporation systems – a review. Appl. Energ. *292*, 116871.

37. Li, S., Liu, J., Yin, Z., Ren, P., Lin, L., Gong, Y., Yang, C., Zheng, X., Cao, R., Yao, S., et al. (2020). Impact of the coordination environment on atomically dispersed Pt catalysts for oxygen reduction reaction. ACS Catal. *10*, 907–913.

38. Li, S., Yang, J., Song, C., Zhu, Q., Xiao, D., and Ma, D. (2019). Iron carbides: control synthesis and catalytic applications in CO_x hydrogenation and electrochemical HER. Adv. Mater. *31*, 1901796.

39. Xu, Y., Zhai, P., Deng, Y., Xie, J., Liu, X., Wang, S., and Ma, D. (2020). Highly selective olefin production from CO_2 hydrogenation on iron catalysts: a subtle synergy between manganese and sodium additives. Angew. Chem. Int. Ed. *59*, 21736–21744.

40. Yan, P., Guo, W., Liang, Z., Meng, W., Yin, Z., Li, S., Li, M., Zhang, M., Yan, J., Xiao, D., et al. (2019). Highly efficient K-Fe/C catalysts derived from metal-organic frameworks towards ammonia synthesis. Nano Res. *12*, 2341–2347.

41. Zhao, H., Liu, J.-X., Yang, C., Yao, S., Su, H.-Y., Gao, Z., Dong, M., Wang, J., Rykov Alexandre, I., Wang, J., et al. (2020). Synthesis of iron-carbide nanoparticles: identification of the active phase and mechanism of Fe-based

fischer–tropsch synthesis. CCS Chem. *2*, 2712–2724.

42. Wu, C., Lin, L., Liu, J., Zhang, J., Zhang, F., Zhou, T., Rui, N., Yao, S., Deng, Y., Yang, F., et al. (2020). Inverse ZrO_2/Cu as a highly efficient methanol synthesis catalyst from CO_2 hydrogenation. Nat. Commun. *11*, 5767.

43. Xu, Y., Li, J., Li, W., Li, W., Zhang, X., Zhao, Y., Xie, J., Wang, X., Liu, X., Li, Y., et al. (2019). Direct conversion of CO and H_2O into liquid fuels under mild conditions. Nat. Commun. *10*, 1389.

44. Mateo, D., Cerrillo, J.L., Durini, S., and Gascon, J. (2021). Fundamentals and applications of photo-thermal catalysis. Chem. Soc. Rev. *50*, 2173–2210.

45. Wang, Z.-j., Song, H., Liu, H., and Ye, J. (2020). Coupling of solar energy and thermal energy for carbon dioxide reduction: status and prospects. Angew. Chem. Int. Ed. *59*, 8016–8035.

46. Xu, M., Hu, X., Wang, S., Yu, J., Zhu, D., and Wang, J. (2019). Photothermal effect promoting CO_2 conversion over composite photocatalyst with high graphene content. J. Catal. *377*, 652–661.

47. Hoch, L.B., Wood, T.E., O'Brien, P.G., Liao, K., Reyes, L.M., Mims, C.A., and Ozin, G.A. (2014). The rational design of a single-component photocatalyst for gas-phase CO_2 reduction using both UV and visible light. Adv. Sci. *1*, 1400013.

48. Zhang, H., Wang, T., Wang, J., Liu, H., Dao, T.D., Li, M., et al. (2016). Surface-plasmon-enhanced photodriven CO_2 reduction catalyzed by metal–organic-framework-derived iron nanoparticles encapsulated by ultrathin carbon layers. Adv. Mater. *28*, 3703–3710.

49. Li, Z., Liu, J., Zhao, Y., Waterhouse, G.I.N., Chen, G., Shi, R., Zhang, X., Liu, X., Wei, Y., Wen, X.-D., et al. (2018). Co-based catalysts derived from layered-double-hydroxide nanosheets for the photothermal production of light olefins. Adv. Mater. *30*, 1800527.

50. Song, C., Liu, X., Xu, M., Masi, D., Wang, Y., Deng, Y., Zhang, M., Qin, X., Feng, K., Yan, J., et al. (2020). Photothermal conversion of CO2 with tunable selectivity using Fe-based catalysts: from oxide to carbide. ACS Catal. *10*, 10364–10374.

51. Xu, C., Zhang, Y., Pan, F., Huang, W., Deng, B., Liu, J., Wang, Z., Ni, M., and Cen, K. (2017). Guiding effective nanostructure design for photo-thermochemical CO_2 conversion: from DFT calculations to experimental verifications. Nano Energy *41*, 308–319.

52. Feng, X., Liu, D., Yan, B., Shao, M., Hao, Z., Yuan, G., Yu, H., and Zhang, Y. (2021). Highly active PdO/Mn_3O_4/CeO_2 nanocomposites supported on one dimensional halloysite nanotubes for photoassisted thermal catalytic methane combustion. Angew. Chem. Int. Ed.

53. Li, Z.-H., Chen, Y., Sun, Y., and Zhang, X.-Z. (2021). Platinum-doped prussian blue nanozymes for multiwavelength bioimaging guided photothermal therapy of tumor and anti-inflammation. ACS Nano *15*, 5189–5200.

54. Wu, Z., Li, C., Li, Z., Feng, K., Cai, M., Zhang, D., et al. (2021). Niobium and titanium carbides (MXenes) as superior photothermal supports for CO_2 photocatalysis. ACS Nano *15*, 5696–5705.

55. Zhang, W., Chen, Y., Zhang, G., Tan, X., Ji, Q., Wang, Z., Liu, H., and Qu, J. (2021). Hot-electron-induced photothermal catalysis for energy-dependent molecular oxygen activation. Angew. Chem. Int. Ed. *60*, 4872–4878.

56. Zhang, Q., Uchaker, E., Candelaria, S.L., and Cao, G. (2013). Nanomaterials for energy conversion and storage. Chem. Soc. Rev. *42*, 3127–3171.

57. Li, S., Xu, Y., Chen, Y., Li, W., Lin, L., Li, M., Deng, Y., Wang, X., Ge, B., Yang, C., et al. (2017). Tuning the selectivity of catalytic carbon dioxide hydrogenation over iridium/cerium oxide catalysts with a strong metal–support interaction. Angew. Chem. Int. Ed. *56*, 10761–10765.

58. Lin, L., Yao, S., Gao, R., Liang, X., Yu, Q., Deng, Y., Liu, J., Peng, M., Jiang, Z., Li, S., et al. (2019). A highly CO-tolerant atomically dispersed Pt catalyst for chemoselective hydrogenation. Nat. Nanotechnol. *14*, 354–361.

59. Yao, S.Y., Zhang, X., Zhou, W., Gao, R., Xu, W.Q., Ye, Y.F., Lin, L.L., Wen, X.D., Liu, P., Chen, B.B., et al. (2017). Atomic-layered Au clusters on alpha-MoC as catalysts for the low-temperature water-gas shift reaction. Science *357*, 389–393.

60. Wang, Q., Nakabayashi, M., Hisatomi, T., Sun, S., Akiyama, S., Wang, Z., Pan, Z., Xiao, X., Watanabe, T., Yamada, T., et al. (2019). Oxysulfide photocatalyst for visible-light-driven overall water splitting. Nat. Mater. *18*, 827–832.

61. Wang, Z., Li, C., and Domen, K. (2019). Recent developments in heterogeneous photocatalysts for solar-driven overall water splitting. Chem. Soc. Rev. *48*, 2109–2125.

62. Yan, Y.B., Chen, J., Li, N., Tian, J.Q., Li, K.X., Jiang, J.Z., Liu, J.Y., Tian, Q.H., and Chen, P. (2018). Systematic bandgap engineering of graphene quantum dots and applications for photocatalytic water splitting and CO_2 reduction. ACS Nano *12*, 3523–3532.

63. Chen, X.B., Liu, L., Yu, P.Y., and Mao, S.S. (2011). Increasing solar absorption for photocatalysis with black hydrogenated titanium dioxide nanocrystals. Science *331*, 746–750.

64. Yin, Z., Wang, Y., Song, C., Zheng, L., Ma, N., Liu, X., Li, S., Lin, L., Li, M., Xu, Y., et al. (2018). Hybrid Au-Ag nanostructures for enhanced plasmon-driven catalytic selective hydrogenation through visible light irradiation and surface-enhanced Raman scattering. J. Am. Chem. Soc. *140*, 864–867.

65. An, H., Li, M., Liu, R., Gao, Z., and Yin, Z. (2020). Design of Ag_xAu_{1-x} alloy/$ZnIn_2S_4$ system with tunable spectral response and Schottky barrier height for visible-light-driven hydrogen evolution. Chem. Eng. J. *382*, 122953.

66. An, H., Xiao, S., Zhao, X., Cao, L., Liu, T., Li, M., Wang, B., and Yin, Z. (2021). Construction of highly efficient photocatalyst with core-shell Au@Ag/C@SiO_2 hybrid structure towards visible-light-driven photocatalytic reduction. Chin. J. Chem. *39*.

67. O'Brien, P.G., Sandhel, A., Wood, T.E., Jelle, A.A., Hoch, L.B., Perovic, D.D., Mims, C.A., and Ozin, G.A. (2014). Photomethanation of gaseous CO_2 over Ru/silicon nanowire catalysts with visible and near-infrared photons. Adv. Sci. *1*, 1400001.

68. Chen, G., Gao, R., Zhao, Y., Li, Z., Waterhouse, G.I.N., Shi, R., Zhao, J., Zhang, M., Shang, L., Sheng, G., et al. (2018). Alumina-supported CoFe alloy catalysts derived from layered-double-hydroxide nanosheets for efficient photothermal CO_2 hydrogenation to hydrocarbons. Adv. Mater. *30*, 1704663.

69. Lee, B.H., Park, S., Kim, M., Sinha, A.K., Lee, S.C., Jung, E., Chang, W.J., Lee, K.S., Kim, J.H., Cho, S.P., et al. (2019). Reversible and cooperative photoactivation of single-atom Cu/TiO_2 photocatalysts. Nat. Mater. *18*, 620–626.

70. Liu, X., Shi, H., Meng, X., Sun, C., Zhang, K., Gao, L., Ma, Y., Mu, Z., Ling, Y., Cheng, B., et al. (2021). Solar-enhanced CO_2 conversion with CH_4 over synergetic NiCo alloy catalysts with light-to-fuel efficiency of 33.8 %. Solar RRL *5*, 2100185.

71. Li, Z., Liu, J., Shi, R., Waterhouse, G.I.N., Wen, X.-D., and Zhang, T. (2021). Fe-based catalysts for the direct photohydrogenation of CO_2 to value-added hydrocarbons. Adv. Energy Mater. *11*, 2002783.

72. Govorov, A.O., and Richardson, H.H. (2007). Generating heat with metal nanoparticles. Nano Today *2*, 30–38.

73. Chen, H., Shao, L., Ming, T., Sun, Z., Zhao, C., Yang, B., and Wang, J. (2010). Understanding the photothermal conversion efficiency of gold nanocrystals. Small *6*, 2272–2280.

74. Baffou, G., Quidant, R., and Girard, C. (2009). Heat generation in plasmonic nanostructures: influence of morphology. Appl. Phys. Lett. *94*, 153109.

75. Gao, W., Gao, R., Zhao, Y., Peng, M., Song, C., Li, M., Li, S., Liu, J., Li, W., Deng, Y., et al. (2018). Photo-driven syngas conversion to lower olefins over oxygen-decorated Fe_5C_2 catalyst. Chem *4*, 2917–2928.

76. Yan, B., Du, C., Lin, Z.Y., and Yang, G.W. (2020). Photothermal conversion assisted photocatalytic hydrogen evolution from amorphous carbon nitrogen nanosheets with nitrogen vacancies. Phys. Chem. Chem. Phys. *22*, 4453–4463.

77. Hu, X., Xu, W., Zhou, L., Tan, Y., Wang, Y., Zhu, S., and Zhu, J. (2017). Tailoring graphene oxide-based aerogels for efficient solar steam generation under one sun. Adv. Mater. *29*, 1604031.

78. Xuan, J., Wang, Z., Chen, Y., Liang, D., Cheng, L., Yang, X., Liu, Z., Ma, R., Sasaki, T., and Geng, F. (2016). Organic-base-driven intercalation and delamination for the production of functionalized titanium carbide nanosheets with superior photothermal therapeutic performance. Angew. Chem. Int. Ed. *55*, 14569–14574.

79. Jia, C., Li, Y., Yang, Z., Chen, G., Yao, Y., Jiang, F., Kuang, Y., Pastel, G., Xie, H., Yang, B., et al. (2017). Rich mesostructures derived from natural Woods for solar steam generation. Joule *1*, 588–599.

80. Liu, G., Niu, P., Sun, C., Smith, S.C., Chen, Z., Lu, G.Q., and Cheng, H.-M. (2010). Unique electronic structure induced high photoreactivity of sulfur-doped graphitic C_3N_4. J. Am. Chem. Soc. *132*, 11642–11648.

81. Lin, H., Wang, X., Yu, L., Chen, Y., and Shi, J. (2017). Two-dimensional ultrathin MXene ceramic nanosheets for photothermal conversion. Nano Lett. *17*, 384–391.

82. Bai, Y., Zhao, J., Feng, S., Liang, X., and Wang, C. (2019). Light-driven thermocatalytic CO_2 reduction over surface-passivated β-Mo_2C nanowires: enhanced catalytic stability by light. Chem. Commun. *55*, 4651–4654.

83. Anasori, B., Lukatskaya, M.R., and Gogotsi, Y. (2017). 2D metal carbides and nitrides (MXenes) for energy storage. Nat. Rev. Mater. *2*, 16098.

84. Naguib, M., Kurtoglu, M., Presser, V., Lu, J., Niu, J.J., Heon, M., Hultman, L., Gogotsi, Y., and Barsoum, M.W. (2011). Two-dimensional nanocrystals produced by exfoliation of Ti_3AlC_2. Adv. Mater. *23*, 4248–4253.

85. He, J.X., Zhang, Z., Xiao, C.H., Liu, F., Sun, H.X., Zhu, Z.Q., Liang, W.D., and Li, A. (2020). High-performance salt-rejecting and cost-effective superhydrophilic porous monolithic polymer foam for solar steam generation. ACS Appl. Mater. Interfaces *12*, 16308–16318.

86. Ha, M.N., Lu, G., Liu, Z., Wang, L., and Zhao, Z. (2016). 3DOM-$LaSrCoFeO_{6-\delta}$ as a highly active catalyst for the thermal and photothermal reduction of CO_2 with H_2O to CH_4. J. Mater. Chem. A *4*, 13155–13165.

87. Yang, M.Q., Gao, M., Hong, M., and Ho, G.W. (2018). Visible-to-NIR photon harvesting: progressive engineering of catalysts for solar-powered environmental purification and fuel production. Adv. Mater. *30*, 1802894.

88. Yang, M.-Q., Shen, L., Lu, Y., Chee, S.W., Lu, X., Chi, X., Chen, Z., Xu, Q.-H., Mirsaidov, U., and Ho, G.W. (2019). Disorder engineering in monolayer nanosheets enabling photothermic catalysis for full solar spectrum (250-2500 nm) harvesting. Angew. Chem. Int. Ed. *58*, 3077–3081.

89. Li, Y., Wen, M., Wang, Y., Tian, G., Wang, C., and Zhao, J. (2021). Plasmonic hot electrons from oxygen vacancies for infrared light-driven catalytic CO_2 reduction on Bi_2O_{3-x}. Angew. Chem. Int. Ed. *60*, 910–916.

90. Zhang, W.B., Wang, L.B., Wang, K.W., Khan, M.U., Wang, M.L., Li, H.L., and Zeng, J. (2017). Integration of photothermal effect and heat insulation to efficiently reduce reaction temperature of CO_2 hydrogenation. Small *13*, 1602583.

91. Zhou, L., Martirez, J.M.P., Finzel, J., Zhang, C., Swearer, D.F., Tian, S., Robatjazi, H., Lou, M., Dong, L., Henderson, L., et al. (2020). Light-driven methane dry reforming with single atomic site antenna-reactor plasmonic photocatalysts. Nat. Energy *5*, 61–70.

92. Méndez-Ramos, J., Acosta-Mora, P., Ruiz-Morales, J.C., Hernández, T., Borges, M.E., and Esparza, P. (2013). Turning into the blue: materials for enhancing TiO_2 photocatalysis by up-conversion photonics. RSC Adv. *3*, 23028–23034.

93. Zhang, M., Lin, Y., Mullen, T.J., Lin, W.F., Sun, L.D., Yan, C.H., Patten, T.E., Wang, D., and Liu, G.Y. (2012). Improving hematite's solar water splitting efficiency by incorporating rare-earth upconversion nanomaterials. J. Phys. Chem. Lett. *3*, 3188–3192.

94. Ren, H., Tang, M., Guan, B., Wang, K., Yang, J., Wang, F., Wang, M., Shan, J., Chen, Z., Wei, D., et al. (2017). Hierarchical graphene foam for efficient omnidirectional solar–thermal energy conversion. Adv. Mater. *29*, 1702590.

95. Zhao, F., Guo, Y., Zhou, X., Shi, W., and Yu, G. (2020). Materials for solar-powered water evaporation. Nat. Rev. Mater. *5*, 388–401.

96. Zhou, C., Yang, Y., Zhu, Y., Ma, J., Long, J., Yuan, R., Ding, Z., Li, Z., and Xu, C. (2018). A graphene-hidden structure with diminished light shielding effect: more efficient graphene-involved composite photocatalysts. Catal. Sci. Technol. *8*, 4734–4740.

97. Fang, Z.C., Wang, Y.C., Liu, C.X., Chen, S., Sang, W., Wang, C., and Zeng, J. (2015). Rational design of metal nanoframes for catalysis and plasmonics. Small *11*, 2593–2605.

98. Liu, H., Ye, H.G., Gao, M., Li, Q., Liu, Z., Xie, A.Q., Zhu, L., Ho, G.W., and Chen, S. (2021). Conformal microfluidic-blow-spun 3D photothermal catalytic spherical evaporator for omnidirectional enhanced solar steam generation and CO_2 reduction. Adv. Sci. 2101232.

99. Peng, M., Dong, C., Gao, R., Xiao, D., Liu, H., and Ma, D. (2021). Fully exposed cluster catalyst (FECC): toward rich surface sites and full atom utilization efficiency. ACS Cent. Sci. *7*, 262–273.

100. Huang, H., Zhang, L., Lv, Z., Long, R., Zhang, C., Lin, Y., Wei, K., Wang, C., Chen, L., Li, Z.-Y., et al. (2016). Unraveling surface plasmon decay in core–shell nanostructures toward broadband light-driven catalytic organic synthesis. J. Am. Chem. Soc. *138*, 6822–6828.

101. Linic, S., Christopher, P., and Ingram, D.B. (2011). Plasmonic-metal nanostructures for efficient conversion of solar to chemical energy. Nat. Mater. *10*, 911–921.

102. Tian, Y., and Tatsuma, T. (2005). Mechanisms and applications of plasmon-induced charge separation at TiO_2 films loaded with gold nanoparticles. J. Am. Chem. Soc. *127*, 7632–7637.

103. Wang, H., Wang, Y., Guo, L., Zhang, X., Ribeiro, C., and He, T. (2020). Solar-heating boosted catalytic reduction of CO_2 under full-solar spectrum. Chin. J. Catal. *41*, 131–139.

104. Sarina, S., Zhu, H.-Y., Xiao, Q., Jaatinen, E., Jia, J., Huang, Y., Zheng, Z., and Wu, H. (2014). Viable photocatalysts under solar-spectrum irradiation: nonplasmonic metal nanoparticles. Angew. Chem. Int. Ed. *53*, 2935–2940.

105. Xiao, J.-D., and Jiang, H.-L. (2019). Metal–organic frameworks for photocatalysis and photothermal catalysis. Acc. Chem. Res. *52*, 356–366.

106. Yang, Q., Xu, Q., Yu, S.-H., and Jiang, H.-L. (2016). Pd Nanocubes@ZIF-8: integration of plasmon-driven photothermal conversion with a metal–organic framework for efficient and selective catalysis. Angew. Chem. Int. Ed. *55*, 3685–3689.

107. Chen, Y.-Z., Wang, Z.U., Wang, H., Lu, J., Yu, S.-H., and Jiang, H.-L. (2017). Singlet oxygen-engaged selective photo-oxidation over Pt nanocrystals/porphyrinic MOF: the roles of photothermal effect and Pt electronic state. J. Am. Chem. Soc. *139*, 2035–2044.

108. Wang, F., Huang, Y., Chai, Z., Zeng, M., Li, Q., Wang, Y., and Xu, D. (2016). Photothermal-enhanced catalysis in core–shell plasmonic hierarchical Cu_7S_4 microsphere@zeolitic imidazole framework-8. Chem. Sci. *7*, 6887–6893.

109. Thommes, M., Kaneko, K., Neimark, A.V., Olivier, J.P., Rodriguez-Reinoso, F., Rouquerol, J., and Sing, K.S.W. (2015). Physisorption of gases, with special reference to the evaluation of surface area and pore size distribution (IUPAC Technical Report). Pure Appl. Chem. *87*, 1051–1069.

110. Wang, Z., Yang, C., Lin, T., Yin, H., Chen, P., Wan, D., Xu, F., Huang, F., Lin, J., Xie, X., et al. (2013). Visible-light photocatalytic, solar thermal and photoelectrochemical properties of aluminium-reduced black titania. Energy Environ. Sci. *6*, 3007.

111. Nicoletti, O., de la Peña, F., Leary, R.K., Holland, D.J., Ducati, C., and Midgley, P.A. (2013). Three-dimensional imaging of localized surface plasmon resonances of metal nanoparticles. Nature *502*, 80–84.

112. Long, R., Li, Y., Song, L., and Xiong, Y.J. (2015). Coupling solar energy into reactions: materials design for surface plasmon-mediated catalysis. Small *11*, 3873–3889.

113. Song, H., Meng, X., Wang, Z.-j., Wang, Z., Chen, H., Weng, Y., Ichihara, F., Oshikiri, M., Kako, T., and Ye, J. (2018). Visible-light-mediated methane activation for steam methane reforming under mild conditions: a case study of Rh/TiO_2 catalysts. ACS Catal. *8*, 7556–7565.

114. Goubert, G., and McBreen, P.H. (2013). In-situ spectroscopic detection of active surface species in asymmetric heterogeneous catalysis. ChemCatChem *5*, 683–685.

115. Fujita, T., Higuchi, K., Yamamoto, Y., Tokunaga, T., Arai, S., and Abe, H. (2017). In-situ TEM study of a nanoporous Ni-Co catalyst used for the dry reforming of methane. Metals *7*, 406.

116. Hammond, C., Forde, M.M., Ab Rahim, M.H., Thetford, A., He, Q., Jenkins, R.L., Dimitratos, N., Lopez-Sanchez, J.A., Dummer, N.F., Murphy, D.M., et al. (2012). Direct catalytic conversion of methane to methanol in an aqueous medium by using copper-promoted Fe-ZSM-5. Angew. Chem. Int. Ed. *51*, 5129–5133.

117. Zhang, L.P., Ran, J.R., Qiao, S.Z., and Jaroniec, M. (2019). Characterization of semiconductor photocatalysts. Chem. Soc. Rev. *48*, 5184–5206.

118. Xie, J., Jin, R., Li, A., Bi, Y., Ruan, Q., Deng, Y., Zhang, Y., Yao, S., Sankar, G., Ma, D., et al. (2018). Highly selective oxidation of methane to methanol at ambient conditions by titanium dioxide-supported iron species. Nat. Catal. *1*, 889–896.

119. Zhang, L., Zhang, Y., Huang, X., Tao, L., and Bi, Y. (2021). Direct observation of dynamic interfacial bonding and charge transfer in metal-free photocatalysts for efficient hydrogen evolution. Appl. Catal. B *283*, 119633.

120. Kennedy, J.C., III, and Datye, A.K. (1998). Photothermal heterogeneous oxidation of ethanol over Pt/TiO_2. J. Catal. *179*, 375–389.

121. Meng, X., Wang, T., Liu, L., Ouyang, S., Li, P., Hu, H., Kako, T., Iwai, H., Tanaka, A., and Ye, J. (2014). Photothermal conversion of CO_2 into CH_4 with H_2 over Group VIII nanocatalysts: an alternative approach for solar fuel production. Angew. Chem. Int. Ed. *53*, 11478–11482.

122. Li, X., Zhang, X., Everitt, H.O., and Liu, J. (2019). Light-induced thermal gradients in ruthenium catalysts significantly enhance ammonia production. Nano Lett. *19*, 1706–1711.

123. Li, X., Zhao, S., Duan, X., Zhang, H., Yang, S.-z., Zhang, P., Jiang, S.P., Liu, S., Sun, H., and Wang, S. (2021). Coupling hydrothermal and photothermal single-atom catalysis toward excellent water splitting to hydrogen. Appl. Catal. B *283*, 119660.

124. Zhou, Y., Ding, T., Gao, M., Chan, K.H., Cheng, Y., He, J., and Ho, G.W. (2020). Controlled heterogeneous water distribution and evaporation towards enhanced photothermal water-electricity-hydrogen production. Nano Energy *77*, 105102.

125. Gu, L., Zhang, C., Guo, Y., Gao, J., Yu, Y., and Zhang, B. (2019). Enhancing electrocatalytic water splitting activities via photothermal effect over bifunctional nickel/reduced graphene oxide nanosheets. ACS Sustain. Chem. Eng. *7*, 3710–3714.

126. Zhao, L., Yang, Z., Cao, Q., Yang, L., Zhang, X., Jia, J., Sang, Y., Wu, H.-J., Zhou, W., and Liu, H. (2019). An earth-abundant and multifunctional Ni nanosheets array as electrocatalysts and heat absorption layer integrated thermoelectric device for overall water splitting. Nano Energy *56*, 563–570.

127. Ye, T.-N., Park, S.-W., Lu, Y., Li, J., Sasase, M., Kitano, M., Tada, T., and Hosono, H. (2020). Vacancy-enabled N_2 activation for ammonia synthesis on an Ni-loaded catalyst. Nature *583*, 391–395.

128. Li, Y.-N., Chen, Z.-Y., Bao, S.-J., Wang, M.-Q., Song, C.-L., Pu, S., and Long, D. (2018). Ultrafine TiO_2 encapsulated in nitrogen-doped porous carbon framework for photocatalytic degradation of ammonia gas. Chem. Eng. J. *331*, 383–388.

129. Tang, P., Zhu, Q., Wu, Z., and Ma, D. (2014). Methane activation: the past and future. Energy Environ. Sci. *7*, 2580–2591.

130. Liu, L., Puga, A.V., Cored, J., Concepción, P., Pérez-Dieste, V., García, H., and Corma, A. (2018). Sunlight-assisted hydrogenation of CO_2 into ethanol and C_{2+} hydrocarbons by sodium-promoted Co@C nanocomposites. Appl. Catal. B *235*, 186–196.

131. Sorcar, S., Hwang, Y., Lee, J., Kim, H., Grimes, K.M., Grimes, C.A., Jung, J.-W., Cho, C.-H., Majima, T., Hoffmann, M.R., et al. (2019). CO_2, water, and sunlight to hydrocarbon fuels: a sustained sunlight to fuel (Joule-to-Joule) photoconversion efficiency of 1%. Energy Environ. Sci. *12*, 2685–2696.

132. Yang, J., Xiao, W., Chi, X., Lu, X., Hu, S., Wu, Z., Tang, W., Ren, Z., Wang, S., Yu, X., et al. (2020). Solar-driven efficient methane catalytic oxidation over epitaxial ZnO/$La_{0.8}Sr_{0.2}CoO_3$ heterojunctions. Appl. Catal. B *265*, 118469.

133. Liu, H.M., Li, M., Dao, T.D., Liu, Y.Y., Zhou, W., Liu, L.Q., Meng, X.G., Nagao, T., and Ye, J.H. (2016). Design of PdAu alloy plasmonic nanoparticles for improved catalytic performance in CO_2 reduction with visible light irradiation. Nano Energy *26*, 398–404.

134. Yu, X., Zholobenko, V.L., Moldovan, S., Hu, D., Wu, D., Ordomsky, V.V., and Khodakov, A.Y. (2020). Stoichiometric methane conversion to ethane using photochemical looping at ambient temperature. Nat. Energy *5*, 511–519.

135. Meng, L., Chen, Z., Ma, Z., He, S., Hou, Y., Li, H.-H., Yuan, R., Huang, X.-H., Wang, X., Wang, X., et al. (2018). Gold plasmon-induced photocatalytic dehydrogenative coupling of methane to ethane on polar oxide surfaces. Energy Environ. Sci. *11*, 294–298.

136. Jiang, H.Y., Peng, X.B., Yamaguchi, A., Fujita, T., Abe, H., and Miyauchi, M. (2019). Synergistic photothermal and photochemical partial oxidation of methane over noble metals incorporated in mesoporous silica. Chem. Commun. *55*, 13765–13768.

137. Li, J., Chen, G., Yan, J., Huang, B., Cheng, H., Lou, Z., and Li, B. (2020). Solar-driven plasmonic tungsten oxides as catalyst enhancing ethanol dehydration for highly selective ethylene production. Appl. Catal. B *264*, 118517.

138. Xu, C.M., He, H., Xu, Z., Qi, C.D., Li, S.Y., Ma, L.L., Qiu, P.X., and Yang, S.G. (2021). Modification of graphitic carbon nitride by elemental boron cocatalyst with high-efficient charge transfer and photothermal conversion. Chem. Eng. J. *417*, 129203.

139. Xiao, Y., Liu, J., Wang, H., Yang, C., Cheng, H., Deng, Y., Cheng, L., and Fang, Y. (2020). Photothermal oxidation of cyclohexane by graphene oxide-based composites with high selectivity to KA oil. Mol. Catal. *493*, 111103.

140. Yu, E., Li, J., Chen, J., Chen, J., Hong, Z., and Jia, H. (2020). Enhanced photothermal catalytic degradation of toluene by loading Pt nanoparticles on manganese oxide: photoactivation of lattice oxygen. J. Hazard. Mater. *388*, 121800.

141. Xie, Z., Duo, Y., Lin, Z., Fan, T., Xing, C., Yu, L., Wang, R., Qiu, M., Zhang, Y., Zhao, Y., et al. (2020). The rise of 2D photothermal materials beyond graphene for clean water production. Adv. Sci. *7*, 1902236.

142. Nam, D.H., De Luna, P., Rosas-Hernandez, A., Thevenon, A., Li, F.W., Agapie, T., Peters, J.C., Shekhah, O., Eddaoudi, M., and Sargent, E.H. (2020). Molecular enhancement of heterogeneous CO_2 reduction. Nat. Mater. *19*, 266–276.